1990

Effects of electrode hole size on the LAMPF polarized ion source

Glen Allen Morris

The University of Montana

EFFECTS OF ELECTRODE HOLE SIZE

ON

THE LAMPF POLARIZED ION SOURCE

bv

Glen Allen Morris

M.S. Mathematics. Univ. of Wisconsin

A thesis submitted to the Department of Physics

in partial fulfillment of the requirements for the

MASTER OF SCIENCE

UNIVERSITY OF MONTANA

1990

Approved by

Mark Jakobson

RJ Hayden

[signature]

Date June 11, 1990

Morris, Glen A.   MS, June 1990   Physics

Effects of Electrode Hole Size on the LAMPF Polarized Ion Source

Director: Hayden, R. J. and Jakobson, M.J.

Some experiments at the Los Alamos Meson Physics Facility (LAMPF) are limited by the intensity of the particle beams used. The proposed LAMPF optically pumped polarized ion beam source should provide a more intense beam if some difficulties can be overcome. A single large (60-mil) hole in each of the source electrodes causes large transverse velocity components in the beam which lead to low beam intensity. Alternatives to the single large hole must be considered.

In this study, we explore the effect of electrode hole size on final beam current and efficiency. Using Monte Carlo simulation, we trace the progress of beam degradation through the ion beam source and quantify the effect of hole size on ion beam source performance. Alternatives to the use of a single large (60-mil) hole in each electrode have been evaluated.

CONTENTS

LIST OF TABLES AND FIGURES.

INTRODUCTION

A. The Proposed LAMPF Polarized Ion Beam Source. The Los Alamos Meson Physics Facility (LAMPF) conducts a variety of experiments using beams of accelerated particles. Many of the experiments utilizing the LAMPF H- polarized beams are limited by the intensity of the beam. The proposed LAMPF optically pumped ion source should provide a more intense beam if some difficulties with the source can be overcome:

1. The beam particles (protons) originate in a source which ejects them with divergent velocity components.

2. In the polarized ion beam source, the particles undergo charge exchanges and pass unavoidably through electric and magnetic fields which produce beam divergence and particle losses.

3. The particle beams are sufficiently intense that space charge effects are not negligible.

It is hoped that shaped magnetic and electric fields can be used to offset the defocussing effects of the sodium cell charge exchangers, space charge, magnetic fringe fields, and other fields.

The standard configuration of the LAMPF polarized ion source is depicted in Figure 1. The ion source, including its magnets, is roughly 15 cm. in diameter and 90 cm. in length. The horizontal line extending from the electron cyclotron resonance (ECR) source on through the ionizer represents the injector line. Ideally, this will coincide with the centerline of the beam.

The ECR source contains a dense ionized gas (plasma) in the magnetic field of the ECR solenoid.* Plasma protons are accelerated into the circular opening of the first electrode.

The electrode structure is shown in Figure 2. Each electrode is a conducting disc perpendicular to the injector line with its cylindrical hole centered about the injector line. The first, the extraction electrode at an arbitrary voltage, is followed by an electrode which can also be set at an arbitrary voltage. The third electrode is at ground potential. Maximum voltage differences are of the order of a few thousand volts. For the voltage settings shown in Figure 1, many protons are lost in the first electrode, but those which clear that electrode are accelerated by the second electrode and generally continue on through the ion source.

* In the ECR source, microwave energy produces the plasma of electrons and protons from hydrogen atoms. The phrase "optical pumping" applies only to the sodium cell charge exchangers, in which laser energy excites electrons to states of lower binding energy. This makes electrons available to passing protons.

There is a version of the LAMPF ion source which works reasonably well with many of the parameters fixed at specific values. Consequently, it is natural to take that system as a standard and vary some of the parameters, always checking to see if improvement has occurred. It is this standard configuration which is shown in Figure 1, and whose parameters are listed in Table I. The four free parameters set conditions in the electrode region. The other parameters remain fixed in this study.

B. This Thesis and Beam Improvement.

This study deals with the design of the electrode structure. In particular, it is concerned with how to reduce the transverse velocity of the protons emerging from the electrodes. The central task is to explore the effects of electrode hole size on the performance of the ion beam source.

Ideally one could determine the effects of various hole sizes by calculating particle trajectories through the ion source. The trajectory of each particle is the solution to equations of motion incorporating the field forces influencing the particle. However, the initial conditions of the particles are unknown.

In this study, initial particle position is chosen randomly over a limited region on a particular plane. Initial velocity is specified in a similar way. By solving the equations of motion for many particles with initial conditions randomly chosen from specified distributions, statistical distributions can be computed which describe the state of the beam particles as they progress along the beam. The precise form and parameters of the initial distribution of transverse velocity and position have not been found to be critical. (See Jakobson (1987) and Hayden (1989).)

This approach is a form of Monte Carlo simulation. Like some other mathematical methods, it is now truly useful because of advances in computer technology.

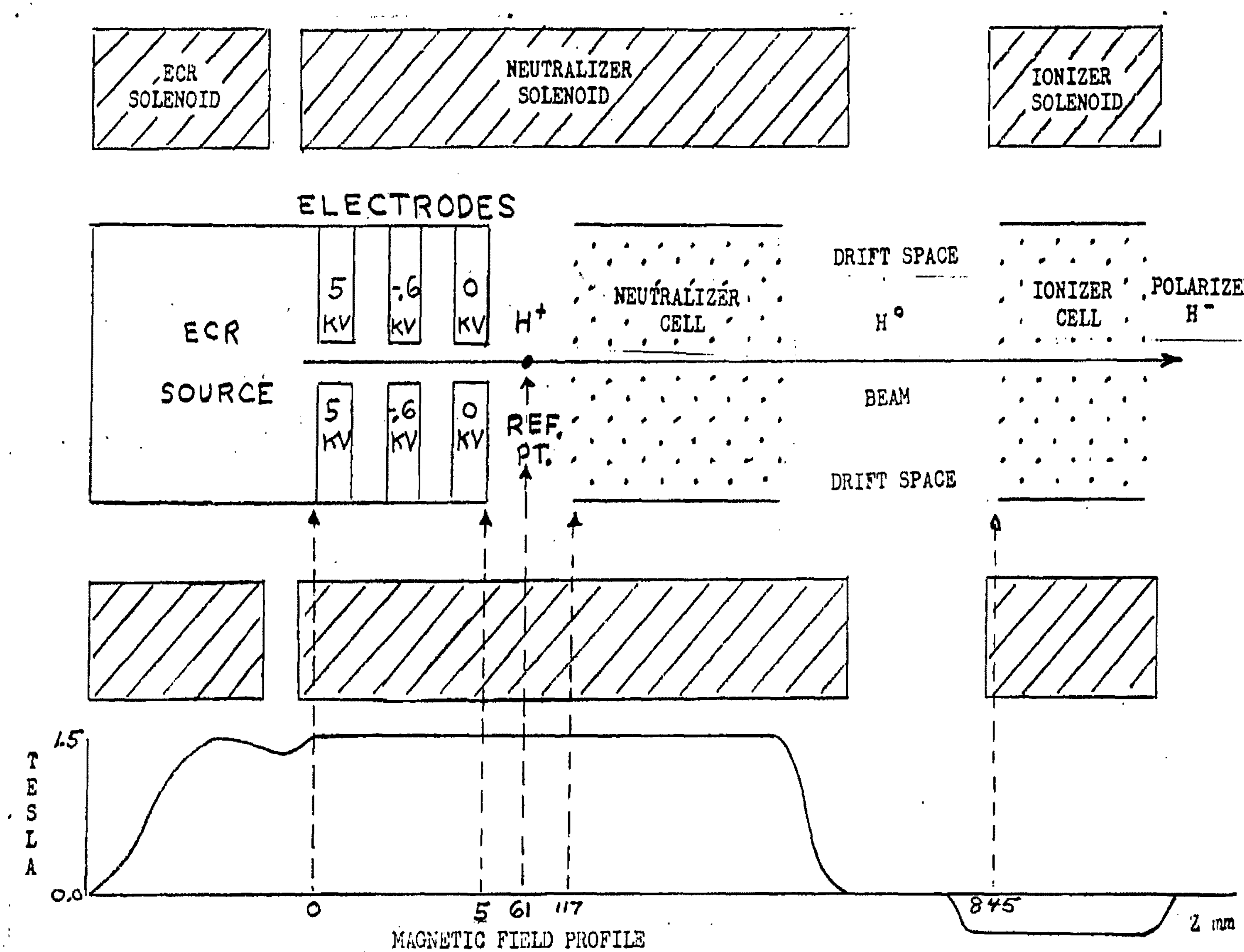

FIG. 1. STANDARD CONFIGURATION OF THE LAMPF ION SOURCE

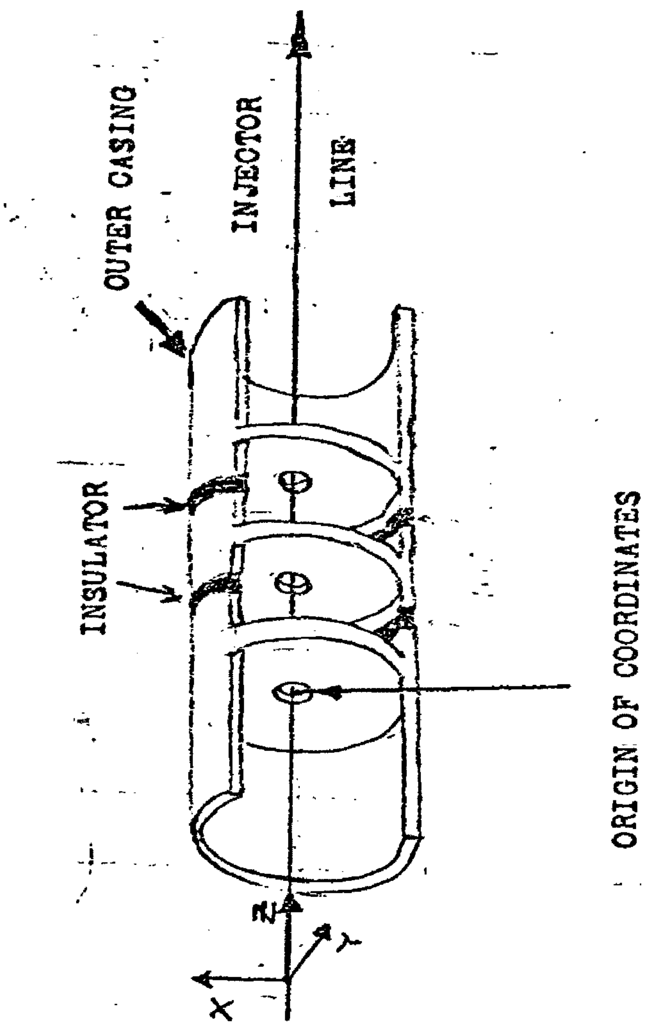

FIG. 2. COORDINATE AXES AND ELECTRODE STRUCTURE

TABLE I. Parameters of the Standard Configuration.

Parameter	Math. Symbol	SCHAR Symbol(s)	Value
Potential on Electrode 1			5000 V
Potential on Electrode 2			-600 V
Potential on Electrode 3			0 V
Axial Magnetic Field near the Electrodes	B_o	B	1.56 T
Radial Magnetic Field near the Electrode			0 T
Initial Proton Speed	V_o	V	1.6E5m/s
Initial Maximum Transverse Speed	$V_\perp(0)$	VSXMAX,VSYMAX	Variable
Diameter of the Electrode Holes	a	XOMAX,YOMAX	Variable
Length of Region 1 (Electrode 1)	T_1	SOUDIS(1)	Variable
Length of Region 2 (Gap)		SOUDIS(2)	.001 m
Length of Region 3 (Electrode 2)		SOUDIS(3)	.001 m
Length of Region 4 (Gap)		SOUDIS(4)	.001 m
Length of Region 5 (Electrode 3)		SOUDIS(5)	.001 m
Distance (Electrodes to Neutralizer)		CELLEN(1)	.112 m
Neutralizer Solenoid Field Length		CELLEN(2)	.0965 m
Drift Region Length		CELLEN(3)	.632 m
Ionizer Solenoid Field Length			
Third Solenoid Hole Radius		RRCUT	.00714 m
Input Current	I_o	CURR	Variable

BACKGROUND

A. Simulating the LAMPF Ion Source. When using computer simulation to study the response of the LAMPF optically pumped ion source to hole size. questions qrise:

1. What coordinate system should be adopted?
2. How many particles should be used in each simulation?
3. What should be the initial position and velocity distribution for the simulation particles?
4. What measures of beam quality can be used to determine the optimum hole size?
5. How should space charge effects be calculated?

This study uses a computer code known as SCHAR (described in Appendix B). How SCHAR deals with these questions is described next.

B. The Coordinate System. The origin of coordinates is at the center of the opening to the first electrode hole. The right handed Cartesian coordinate axes are shown in Figure 2. The z-axis points along the centerline through the electrode holes.

C. Macroparticles and Macrofilaments. In computer simulation of ion beams the particles are represented by macroparticles or macrofilaments. Each macrofilament represents a given fraction of the beam charge. The equations of motion are solved for each particle. The number (N_o) of these particles should be large enough to be sufficiently representative, yet conservative of computer time. If space charge is considered, computer time is proportional to the square of N_o. Experience or testing is required to chose this number.

SCHAR has a mode of calculation, called the line mode, which is used for calculating the space charge force on a particle. In this mode the beam is considered to be composed of infinitely long charged filaments, called macrofilaments. Each macrofilament is fixed in time, lies parallel to the z-axis, at the x,y-position of a particle.

D. Simulating ECR Source Effects. SCHAR simulates the effect of the ECR source by

(1) using KV or parabolic distributions to assign initial conditions (at z=0) to the N particles over an ellipsoid in $X\dot{X}Y\dot{Y}$-space, and

(2) assuming the particles all have the same speed.

The version of SCHAR used offers only the KV distribution. A KV distribution is one in which the particles are uniformly distributed over an area in X,Y(real)-space, an area in $X\dot{X}$ phase space, an area in $Y\dot{Y}$ phase space, and an area in $\dot{X},\dot{Y}$(real)-space. (See Kapchinskij, 1959.) In this study the X,Y and $\dot{X},\dot{Y}$ elliptical areas are initially circular. The initial particle speed is $1.6 * 10^5$ m/s.

E. Beam Quality Parameters. Perhaps the ideal measure of beam quality at an axial coordinate (z) would be the Liouville volume of the swarm of points representing the particles in XPxYPy-space. Here Px and Py are the generalized momenta. In this space the volume of an initially KV-distributed swarm usually remains ellipsoidal. In addition, if the particles do not interact, the density of points in the 4-dimensional volume would remain constant by Liouville's theorem. However, volumes in $XP_x YP_y$ phase space cannot be measured. For this reason, SCHAR uses the spatial derivatives $X'=dX/dZ$ and $Y'=dY/dZ$, and tracks the beam quality in XX'-space and in YY'-space.

In each of these planes SCHAR uses two types of volumes which can be used to describe beam quality:

1. E-volumes and
2. S-volumes.

E-volume measures are areas of 2-dimensional convex regions in the spaces of XX' and YY'. S-volumes are statistical measures of beam quality.

In this study, SCHAR provides emittance (S-volume) as a measure of beam quality. Emittance is most clearly defined in 2 dimensions in a coordinate system rotated so that $\sum_{K=1}^{N} X_K X_K'$ and $\sum_{K=1}^{N} Y_K Y_K'$ are zero. SCHAR defines the X and Y emittances in this case as

$$\epsilon_x = 4\pi X_{rms} X'_{rms}, \text{ and}$$

$$\epsilon_y = 4\pi Y_{rms} Y'_{rms}.$$

X-emittance is, then, the area of an ellipse having semi axes $2X_{rms}$ and $2X'_{rms}$.

At times, particle interactions or non-linear fields influence the particle motions to the extent that these initially ellipsoidal phase space projections become nonellipsoidal. Another possibility is that the particles may not be distributed uniformly in these phase spaces. In either instance, the emittance will not equal the projected area of the particle swarm. For this reason, emittance must be interpreted carefully. If, on the other hand, the phase space distribution is uniform and ellipsoidal, the emittance equals the projected area.

In the software, an unrotated coordinate system is used and so emittance must be calculated by a more general equation. This is discussed in Appendix B.

Another important component of beam quality is total current, which relates directly to the number (N) of particles left in the beam. SCHAR keeps track of N. From the current (I_o) input to the first electrode hole, the current per macrofilament (I_o/N_o) can be used to calculate the beam current at z:

$$I(z) = I_o(N(z)/N_o), \text{ where}$$

$$N = N(z) = \text{number of remaining macrofilaments at } z.$$

F. Calculating Space Charge Effects. A particle will be subject to the electric field force set up by the macrofilaments. This simulates the space charge force on each particle. For each particle SCHAR considers the forces between that particle and the macrofilaments which correspond to the other particles. The sum of these forces is the space charge force on the particle. The sum of this force and the other field forces determines the path of the particle. Thus a charge-carrying entity is considered to be a filament carrying a significant fraction of the total current as far as its effects on other entities is concerned. When its motion is being calculated, the same entity is considered to be a particle (in the electrode region, a proton).

PROBLEM STATEMENT

All but four of the design parameters of the standard electrode structure have a fixed value. The four free parameters are:

$V_\perp(0)$ = maximum transverse speed at z=0

T_1 = thickness of the first electrode

a = the diameter of each electrode hole

I_0 = current input to the electrode structure.

In this study, we discover how effective the standard ion source is when these four parameters are varied.

The questions of primary interest are:

1. How much beam current can the standard ion source transmit at certain settings of ($V_\perp(0)$, T_1, a, I_0) ?

2. Which hole size allows the standard ion source to transmit maximum current in the beam ?

3. For each setting of ($V_\perp(0)$, T_1, a), what input current leads to maximum output current ?

4. What limits the output current ?

Efficiency of transmission is of less concern, but will be considered. One measure of efficiency is N_f/N_0, where N_f is the final number of particles left in the beam. The questions concerning efficiency are:

5. For each setting of ($V_\perp(0)$, T_1, a), what input current leads to a maximum value of N_f/N_0 ?

6. What limits the maximum value of N_f/N_0 ?

METHOD OF SOLUTION

Appendix A describes the computer program POISSON. Because of the cylindrical symmetry of the electrode structure used, the electric field which it generates can be readily calculated by POISSON.

Appendix B describes the space charge simulation program SCHAR. Using SCHAR, it is possible to simulate the dynamics of an ion beam subject to the fields calculated by POISSON or obtained by some other means (York, 1989). The magnetic field due to the first solenoid can be regarded as axial and nearly uniform in the electrode region (Hayden, 1989). Its strength (1.56 T) is a SCHAR input.

Used together, POISSON and SCHAR provide a fairly accurate model for beam dynamics. If the distributions of position and velocity at z=0 are approximated, much can be learned about an ion source through computer simulation. This approach was applied to the LAMPF optically pumped ion source in an effort to answer the questions posed.

Conditions at z=0 were approximated in each case by an appropriate KV distribution. The conditions bounding this distribution are

$$(X_o / X_o^*)^2 + (Y_o / Y_o^*)^2 \leq 1$$

$$(\dot{X}_o / \dot{X}_o^*)^2 + (\dot{Y}_o / \dot{Y}_o^*)^2 \leq 1$$

$$\sqrt{\dot{X}_o^2 + \dot{Y}_o^2 + \dot{Z}_o^2} = V_o \text{ , where}$$

(X,Y,Z) is position and

$(\dot{X}, \dot{Y}, \dot{Z})$ is velocity.

In this study,

$X_o = Y_o = a/2$ (electrode aperture radius),

$\dot{X}_o^* = \dot{Y}_o^* = V_\perp(0)$, and

$V_o = 1.6 * 10$ m/s.

With initial conditions thus specified, POISSON and SCHAR were then used with various values of the four free parameters.

The parameter variations were as follows:

1. Six electrode hole sizes, that is,

   a = 10, 20, 30, 40, 50, or 60 mils.

2. For each hole size, 5 to 11 levels of input current (I_o).

3. Initial maximum transverse speed ($V_\perp(0)$) and first electrode thickness (T_1) took on the following values.

   $V_\perp(0)$ = 30000 m/s, T_1 = .001 m

   $V_\perp(0)$ = 60000 m/s, T_1 = .001 m

   $V_\perp(0)$ = 30000 m/s, T_1 = .0016 m.

In other words, SCHAR was run for several input current levels for each of the 18 combinations of $V_\perp(0)$, T_1 and a, a total of 110 SCHAR runs. (In contrast, a single geometry change with the actual ion beam source may require a month of technician time for disassembly, modification, assembly, evacuation, and startup.)

POISSON takes the electrode voltages and geometry map (which includes T_1 and a), then calculates and stores a grid of electric field values. SCHAR then uses the stored electric field values, and accepts, from the keyboard, the maximum transverse speed $V_{\perp}(0)$ and the input current (I_o). The other program inputs, including the magnetic field strength, were set according to Table I. The initial number (N_o) of particles was 1000. SCHAR then assigned random initial conditions to these particles, in accordance with the KV distribution.

Beginning at z=0, which is at the first electrode hole opening, SCHAR integrates the equations of motion, progressing axially, with z as an independent variable, through the electrode region and on through the rest of the ion source. At certain values of z, SCHAR provides output characterizing the locations and motions of the particles. If the macrofilaments are sufficiently numerous and initialized with an appropriate distribution of positions and velocities, this output should match the statistics of real ion beams.

The most important outputs were:

$V_{\perp}$ = rms transverse speed,

N = number of macrofilaments left,

ϵ_x = XX′ emittance,

ϵ_y = YY′ emittance.

Monitoring occurred at the following axial locations* (z):

z = 1 mm, the exit from the first electrode,
z = 2 mm, the entrance to the second electrode,
z = 3 mm, the exit from the second electrode,
z = 4 mm, the entrance to the third electrode,
z = 5 mm, the exit from the third electrode,
z = 61 mm, an arbitrary reference point, and
z = 845 mm, the entrance to the ionizer.

This study is primarily concerned with final beam current (I_f). That quantity is calculated by multiplying the average final macrofilament count ($\overline{N_f}$) by the current-per-macrofilament (I_o/N_o). SCHAR allows convenient run-replication to obtain a statistically stable value of $\overline{N_f}$.

For each combination of $V_\perp(0)$, T_l, a, and I_o, the beam responses were tabulated. Plots of current, current density, and the ratio N_f/N_o were then prepared to help answer the questions posed.

* If the thickness of the first electrode is changed, the monitoring locations are shifted along the axis a corresponding distance.

RESULTS.

Performance Characteristics. The simulations show that. for any of the 6 hole sizes, the maximum final beam current is obtained when $V_{\perp}(0) = 30000$ m/s and $T_1 = .001$ m. (See Figure 3.) Consequently, in the interpretations that follow, it will be assumed that those conditions hold.

For the 40-mil, 50-mil, and 60-mil hole diameters, Figure 3 shows that the maximum beam current varies roughly as the square of hole diameter. Consequently, if an arrangement with two 40-mil holes per electrode were operated for maximum beam current, that arrangement would deliver nearly as much current as an arrangement with one 60-mil hole in each electrode. A multihole arrangement of 30-mil holes could also replace the single 60-mil hole per electrode. But Figures 4 and 7 show that the current density delivered by the 30-mil hole is much lower: about nineteen (19) holes of that size per electrode would be required to compete with a single 60-mil hole per electrode.

While Figure 3 indicates the limiting current for each setting of ($V_{\perp}(0)$, T_1, a), Figures 5a and 5b indicate how to set the input current to achieve maximum output. For example. for $V_{\perp}(0)=30000$ m/s and $T_1 =.001$ m, the 30-mil hole delivers maximum beam current when $I_0 = 9$ ma.

Figure 6 shows how to achieve maximum efficiency (N_f/N_o). Using the larger hole diameters, maximum efficiency is achieved at an input current which is comparable to the input current which produces maximum current output. For small holes, the simulations show that N_f/N_o rises with decreasing current but never peaks.

Discussion. The final beam current is

$$I_f = I_o (N_f/N_o).$$

According to the simulations, as source current increases, N_f/N_o may peak but then begins to decrease at a finite source current. This is shown in Figure 6. Beam current also begins to diminsh at some level of source current and finally becomes very small. This is shown in Figure 5.

The beam current and efficiency eventually drop with increasing I_o because of particle losses. Factors possibly involved in these losses are:

- initial radial displacement ($R_o = R(Z=0)$)
- initial radial velocity ($\dot{R}_o = \dot{R}(Z=0)$)
- space charge
- radial electric fields
- axial magnetic field (1.56 T)
- axial particle velocity

Other fields present, but not listed here, are negligible. An idea of the importance of each of the listed factors can be obtained by studying SCHAR simulation data obtained for the electrode region.

Figure 8 shows that, in the maximum current mode of operation, at least 70 % of the SCHAR particles are lost in the first electrode, that is, in the interval $z \leqslant 1$ mm. The reason for these losses is suggested, in the figure, by the decreasing number of particles left in the beam at $z = 1$ mm, as input current is increased. For each hole size, increasing input current increases the initial space charge. The SCHAR data verify, then, that space charge is instrumental in the loss of particles in the first hole, regardless of hole size.

Magnetic effects might also become more important as space charge goes up. Magnetic effects, space charge, and initial conditions contribute to accelerations that drive protons into the electrodes.

These factors are resisted by one thing - the inward radial electric field near the first electrode. However for most locations in the first hole, the inward electric field decreases with hole size. (See Figures 13 through 16.) Consequently, for the same input current density, the number of particles lost in the first electrode increases with decreasing hole diameter. This may explain, in part, why the small holes ($a < 40$ mils) cannot pass as much density of current as can larger holes.

Protons in the beam emerging from the first hole are subjected to a forward- and inward-accelerating field. (See Figures 9 and 10.) Consequently, they almost always clear the second electrode. This is why Figure 8 shows so few losses in the interval $2 \lesssim z \lesssim 3$ mm.

Using a 40-mil, 50-mil, or 60-mil hole diameter, and maximum current mode of operation, very few protons are lost at the second electrode and none are lost at the third electrode. The converging forward-accelerating electric field at the right end of the first hole accelerates the protons inward and forward to the extent that they clear the following electrodes. (See Figures 9-16.) The radial component of this focussing field is relatively strong in the larger holes and this may explain why maximum current and efficiency are both achieved at relatively high input currents for hole diameters exceeding 30 mils. (See Figures 5 and 6.)

For these larger holes, the dotted curves in Figure 8 show that, when space charge is ignored, few simulation particles are lost in the first electrode. This confirms that space charge causes most of the divergence and particle losses when the hole diameter exceeds 30 mils.

Using small holes ($a < 40$ mils) and maximum current mode, a substantial percentage of the particles arriving at electrode 3 are lost in that electrode, and the same is true at the first electrode. While this must be partly due to space charge, the dotted curves show that that would occur at both electrodes even if space charge were absent. Thus one or more of the other listed factors is possibly instrumental in the loss of particles to the first and third electrodes when these small diameters are used. The inward electric field is a possible contributor to particle losses: many protons, accelerated inward, can cross the beam and become divergent.

Because of the low diameter-to-length ratio of the small holes and perhaps because of the relative weakness of their inward electric field, maximum efficiency (N_f/N_o) cannot be achieved with them at any input current. This is in contrast to the use of large holes (a > 40 mils) for which maximum current and efficiency both occur at high input current.

Error bars have not been indicated on the graphs. Systematic errors predominate over statistical errors. The effect of hole size and initial electrode shape on the ECR source plasma is an important factor which has not been modelled. Large hole sizes will perturb the plasma.

FIG. 3. Effect of $V_\perp(0)$, T_1, and a on Limiting Current

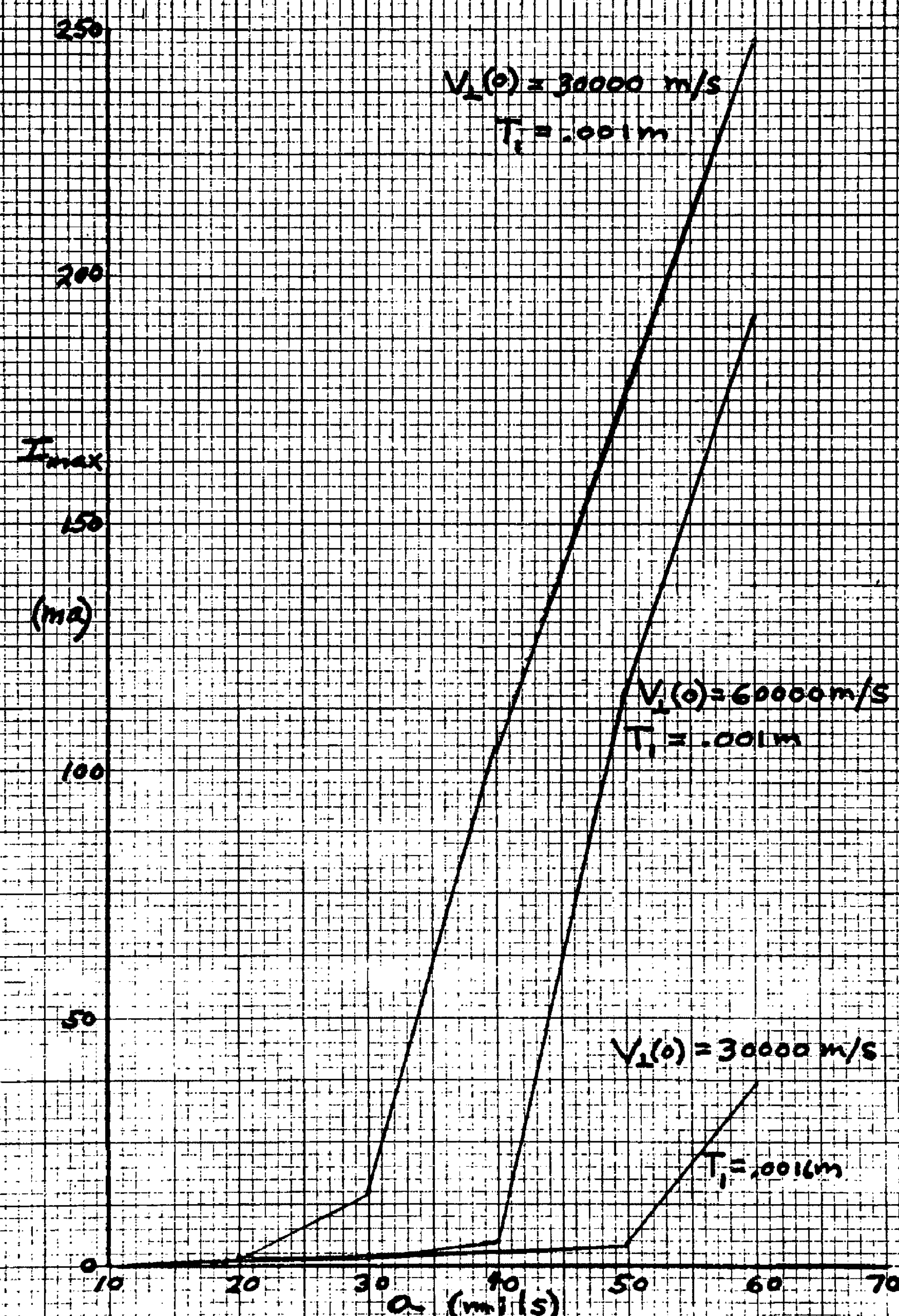

FIG. 4. Output Current Density (i_f) vs. Hole Diameter (a)

(Maximum Current Mode)

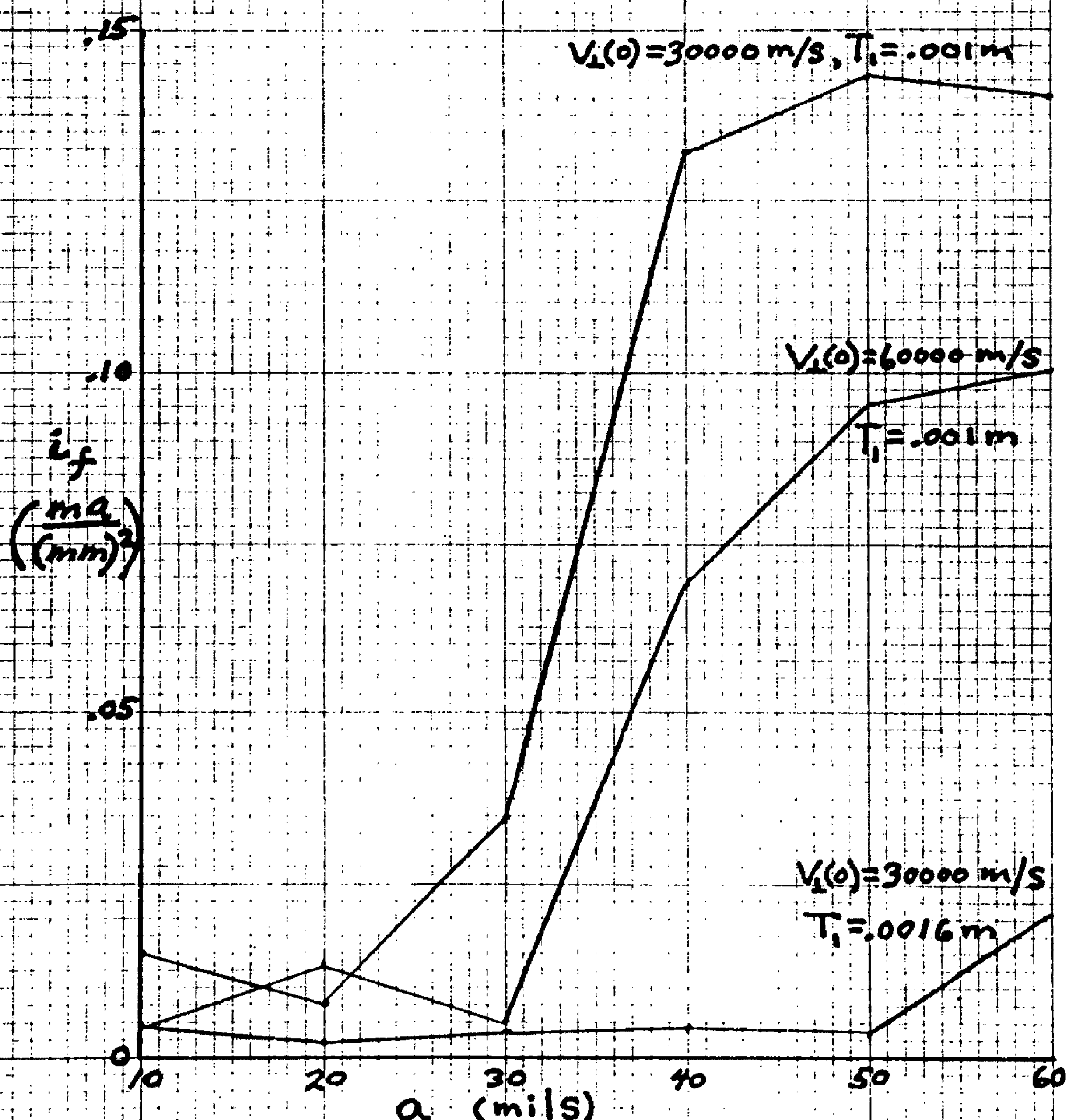

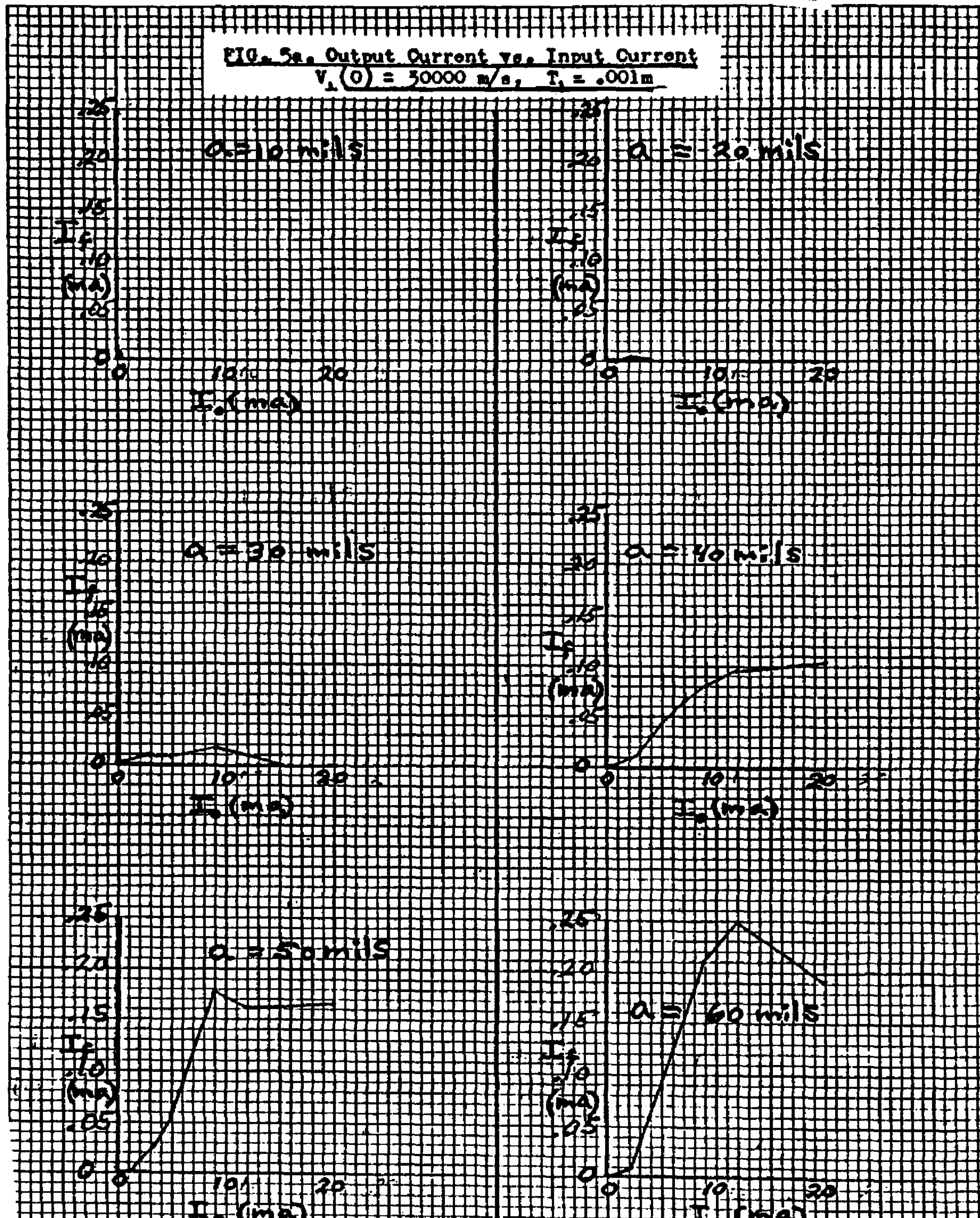
FIG. 5a. Output Current vs. Input Current
$V_1(0)$ = 30000 m/s, T_1 = .001m
a = 10 mils
a = 20 mils
a = 30 mils
a = 40 mils
a = 50 mils
a = 60 mils
I_f (ma)
I_o (ma)

FIG. 5b. Output Current vs. Input Current for Small Holes.
Expanded Scale. $V_1(0) = 30000$ m/s. $T_1 = .001$ m

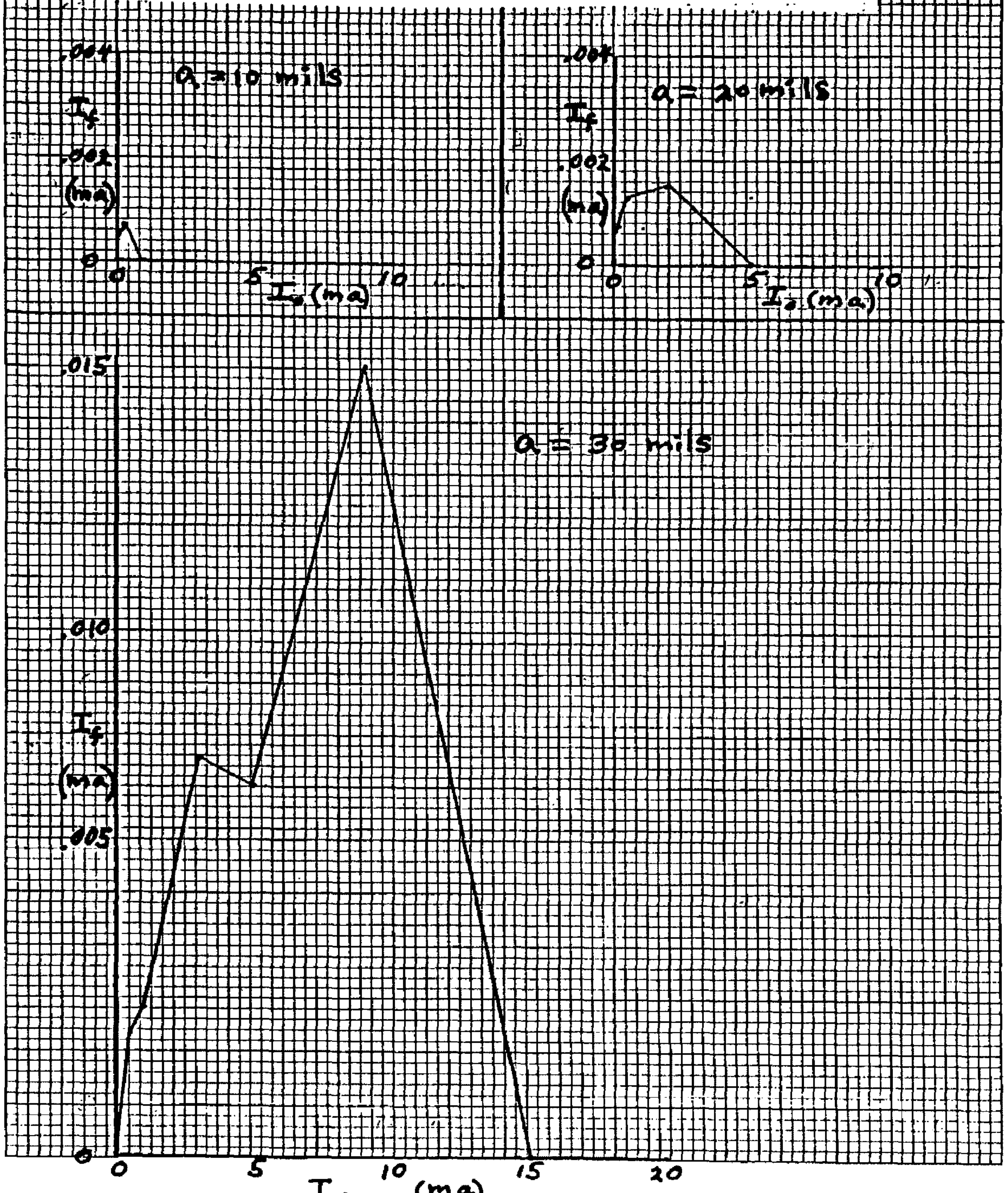

FIG. 6. Final Fraction of Particles Remaining in the Beam.

Note: $N_f = (I_f/I_o)\cdot 1000$ for non-zero space charge

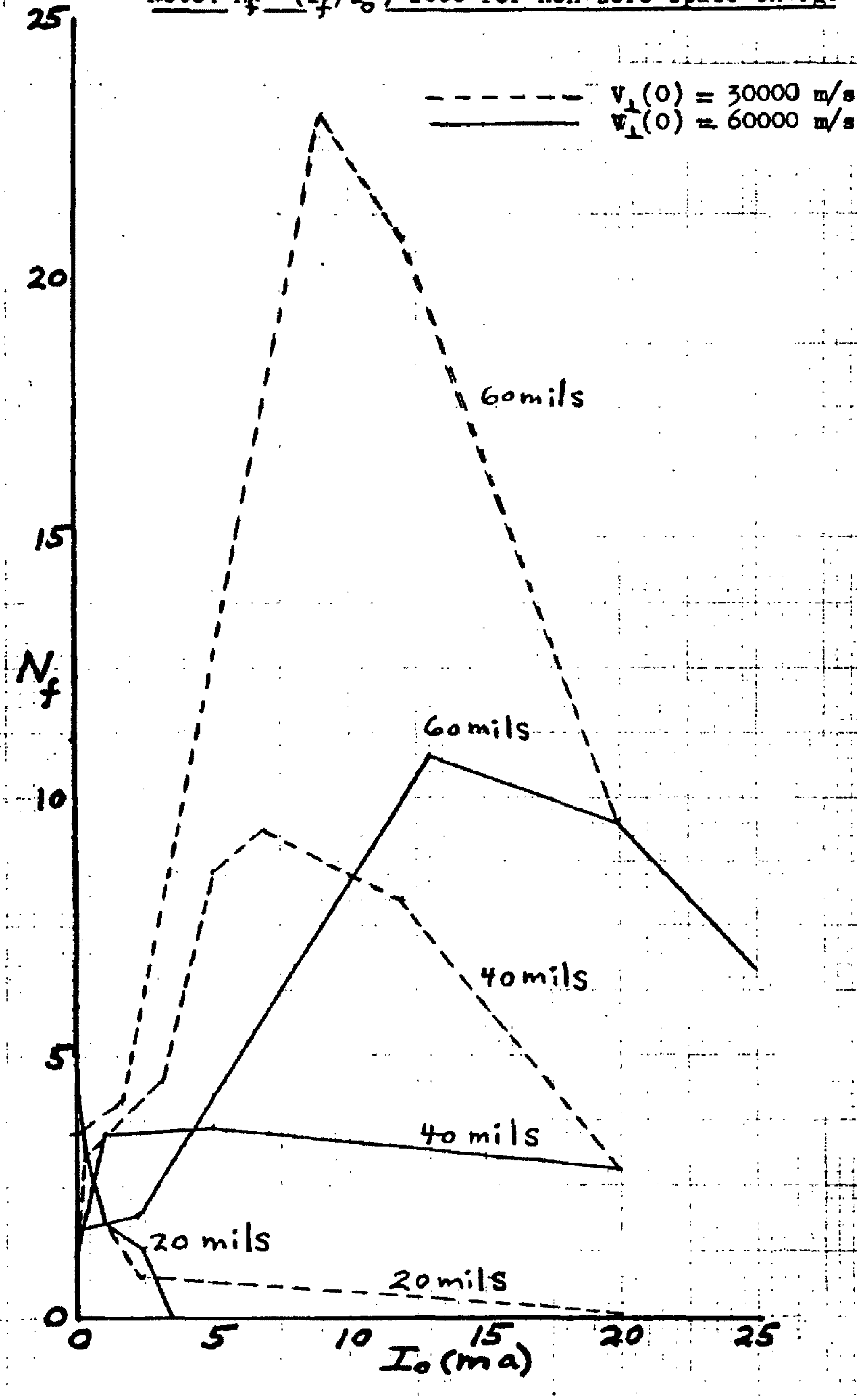

FIG. 7. Final Beam Current Density ($i_f = 4I_o / (\pi a^2)$)
Scale expanded to show beam response at small input currents

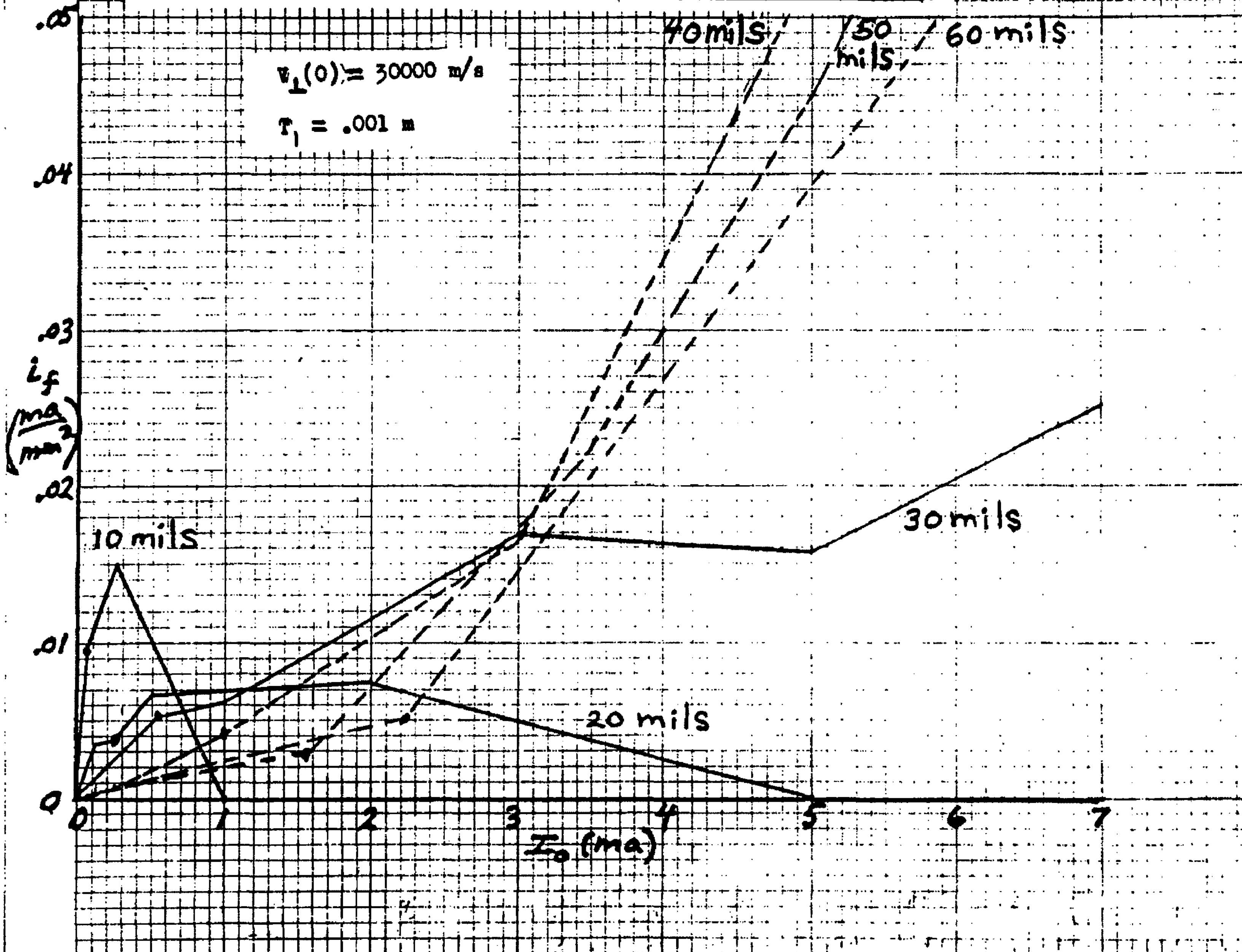

Figure 8. Macroparticle count (N) near the electrode holes. $V_1(0) = 30000$ m/s, $T_i = .0016$ m

I_o = General input current

I_L = Value of I_o which maximizes output current

I_p = Value of I_o which maximizes efficiency (N_f/N_o)

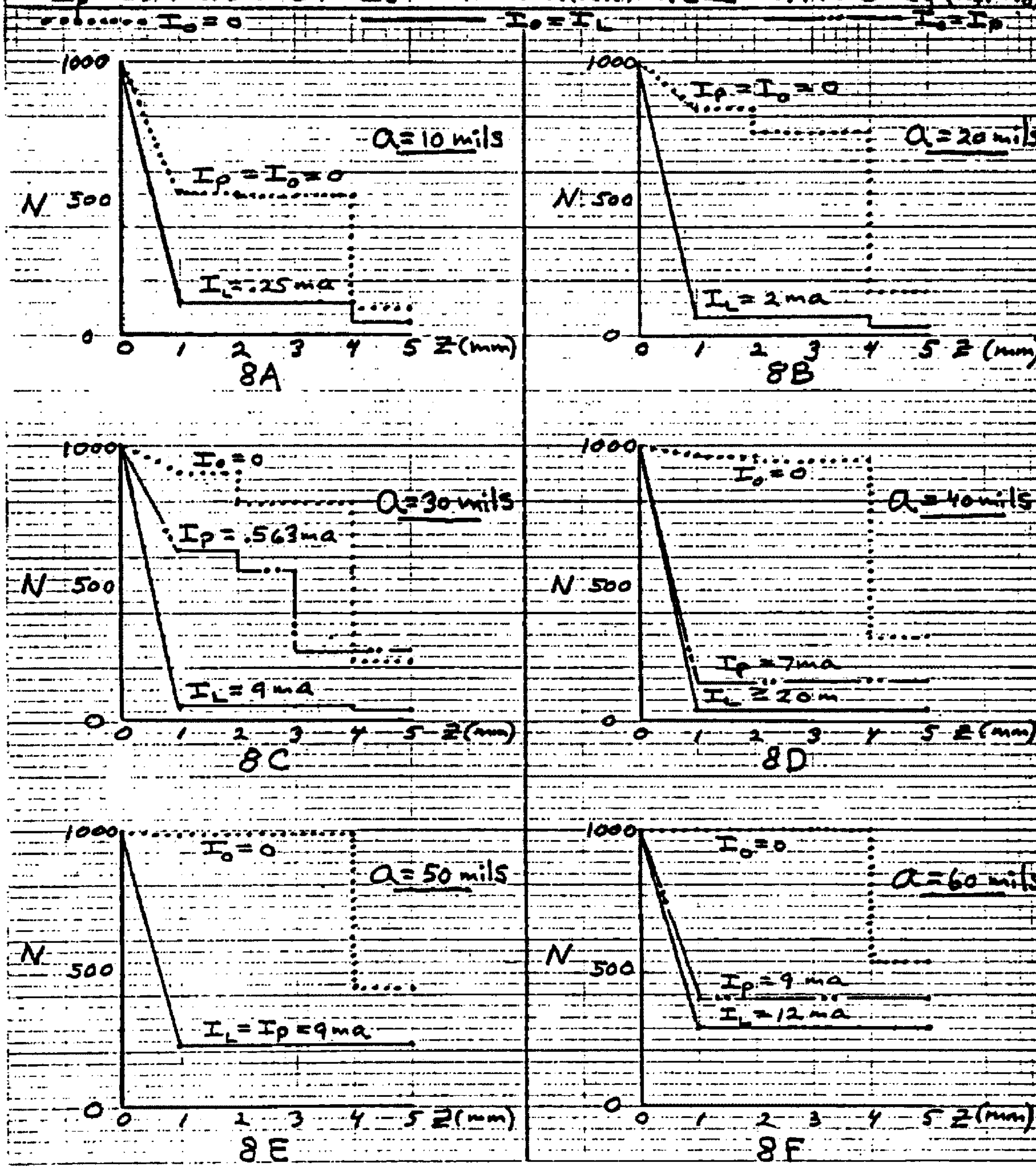

FIG. 9. Equipotential and Electric Field Lines Near the Electrodes
(Hand-drawn for a large hole size.)

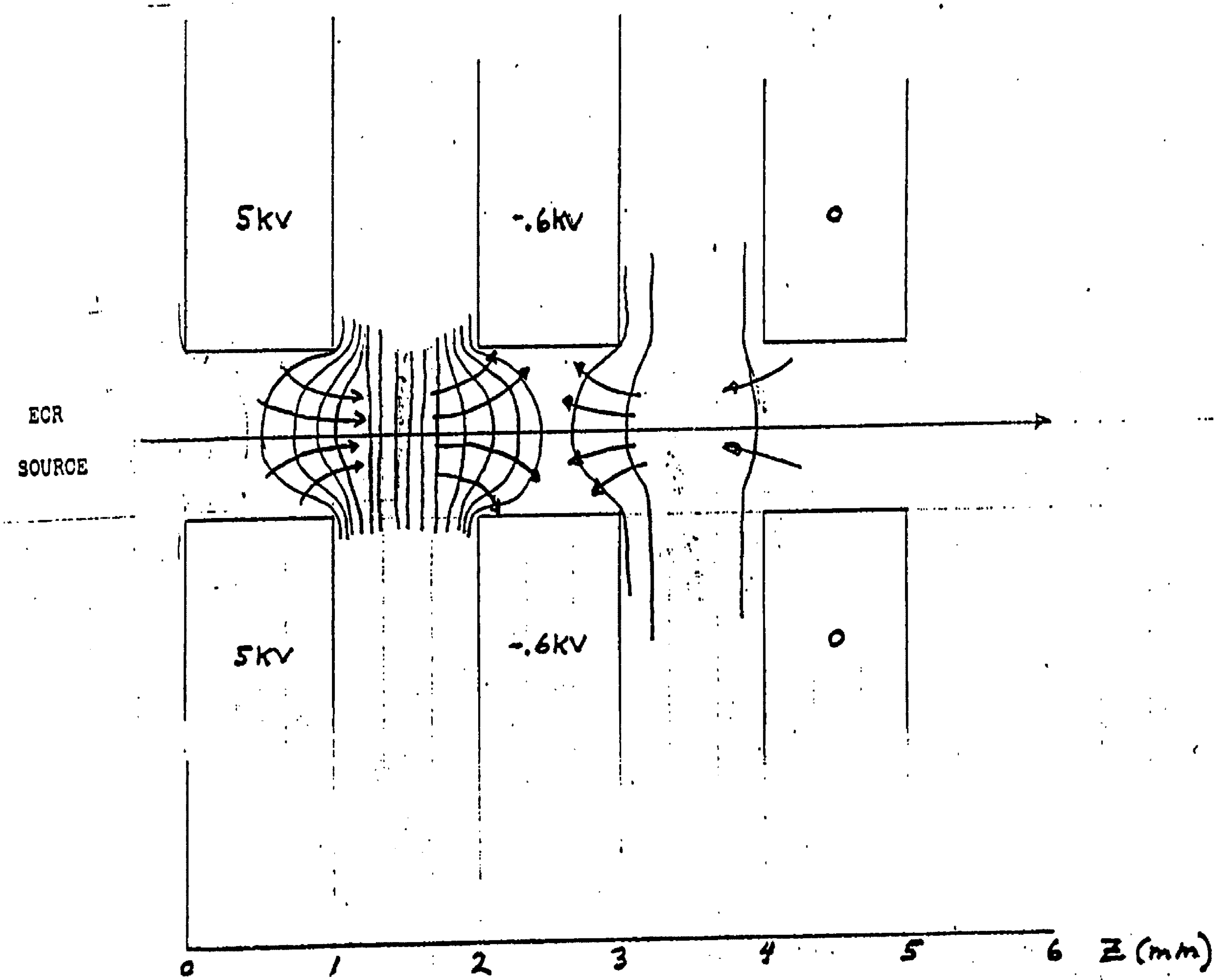

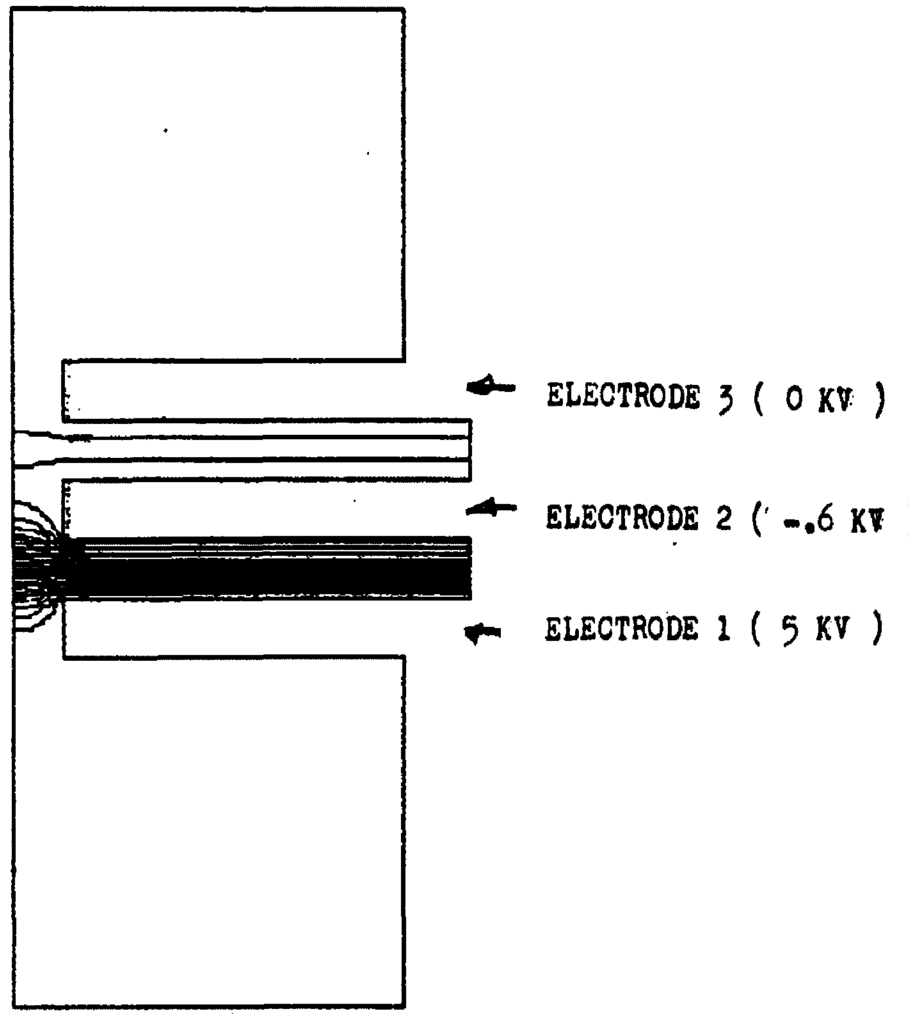

FIG. 10 Equipotential Surfaces due to the Electrode Potentials. The z-axis of the source lies along the left side of the figure. The electrode hole size is 60 mils.

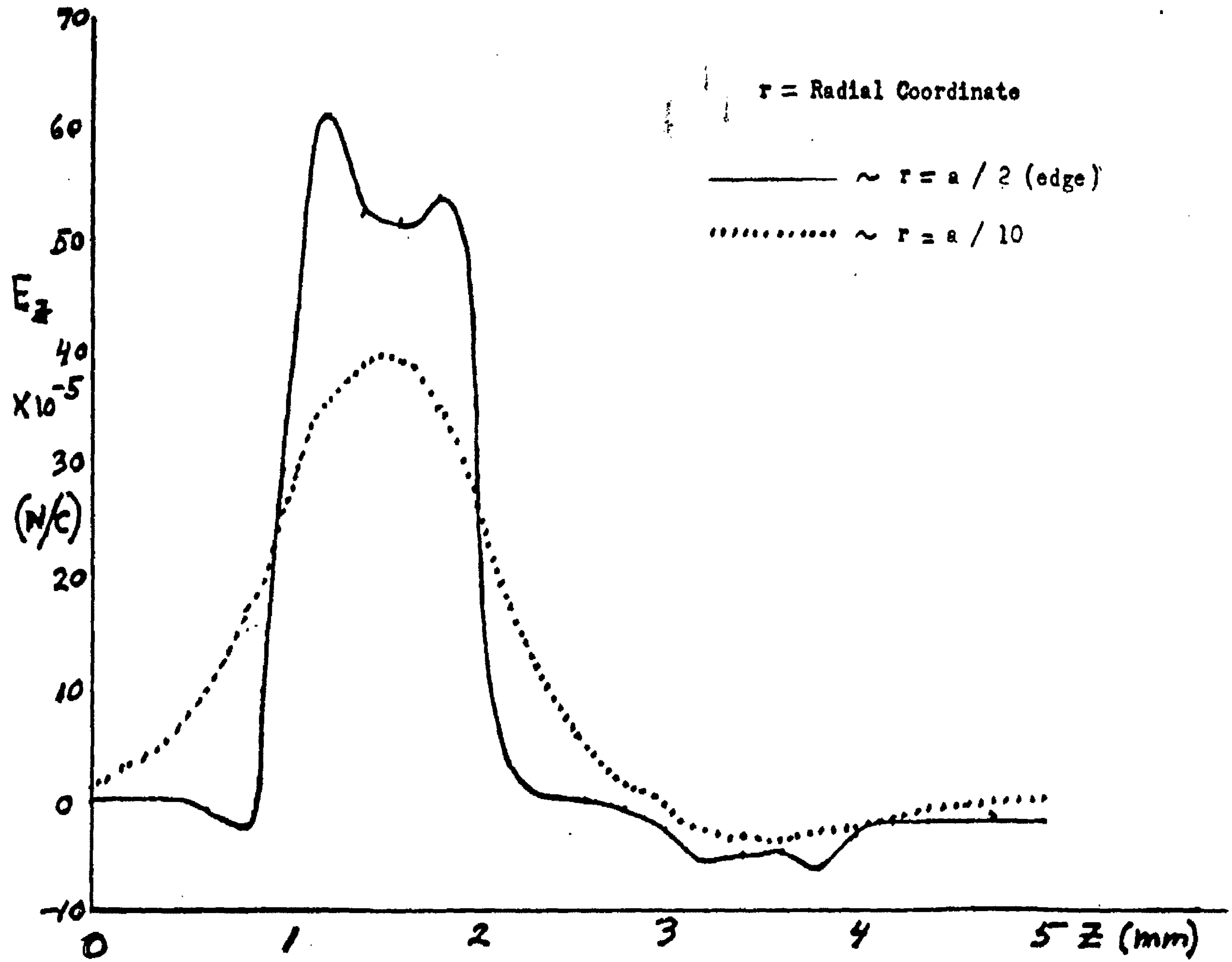

FIG. 11. Axial Electrode Fields Near the Injector Line in the Electrode Region (a = 60 mils)

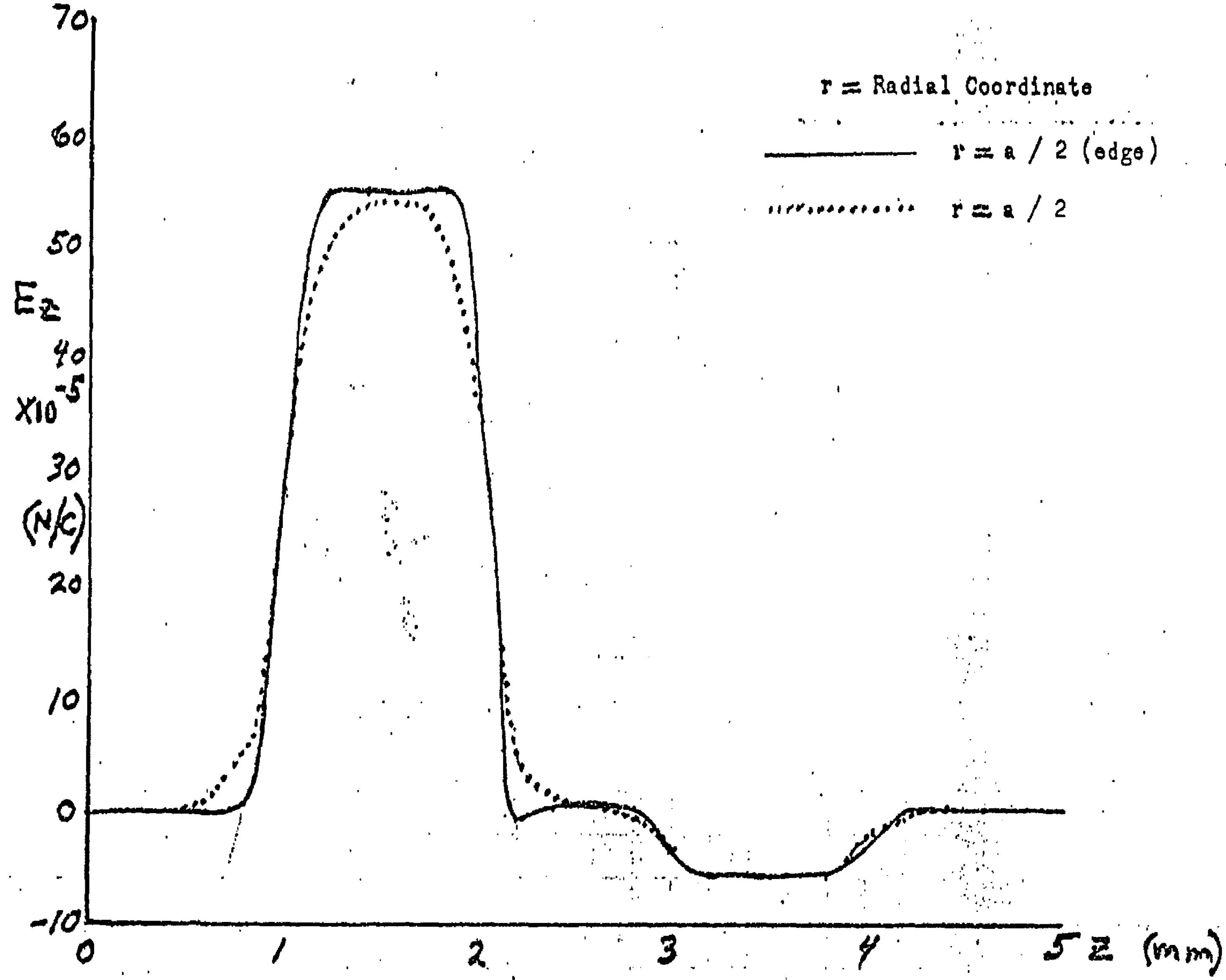

FIG. 12. Axial Electric Fields Near the Injector Line in the Electrode Region (a = 20 mils)

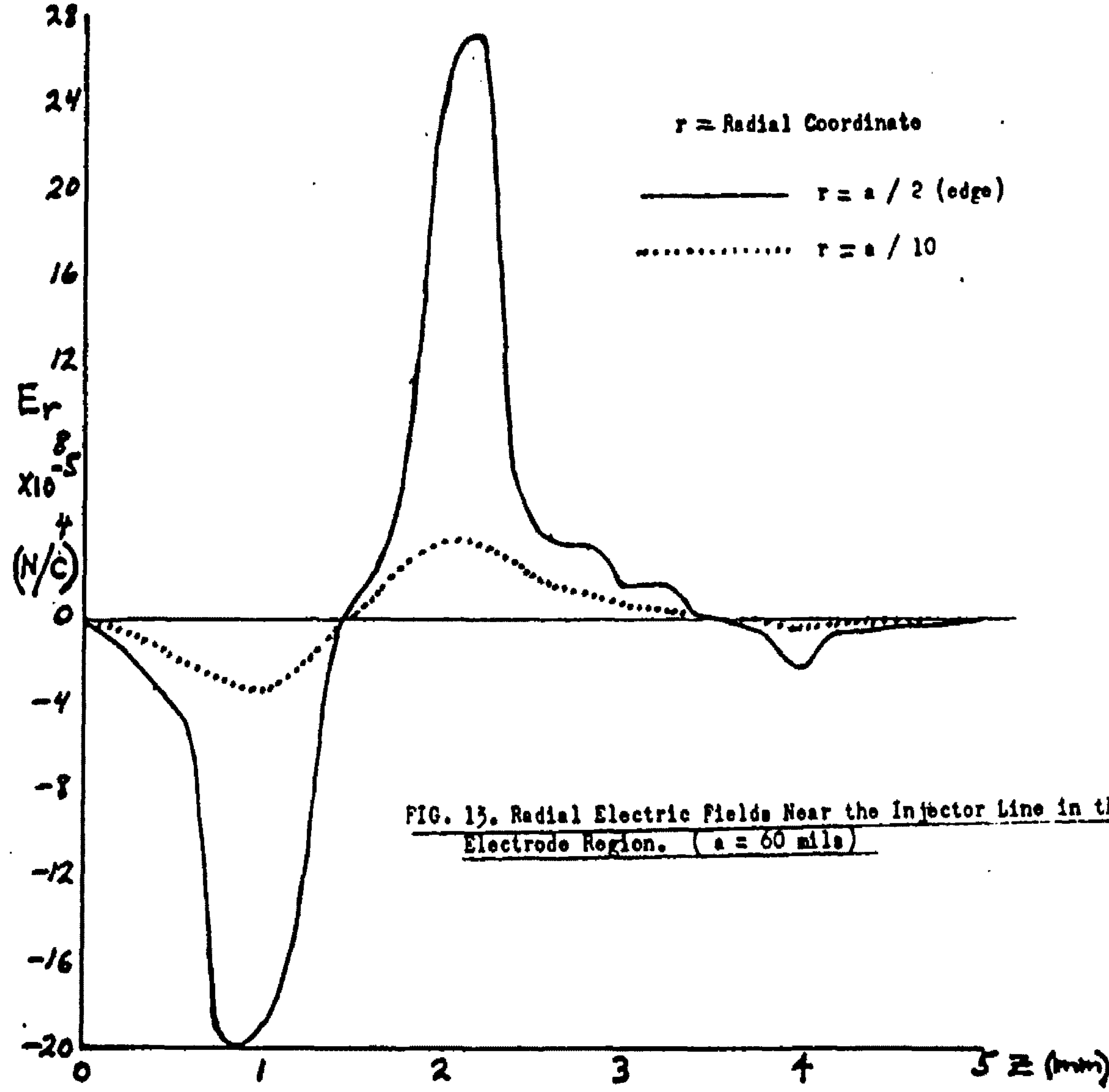

FIG. 13. Radial Electric Fields Near the Injector Line in the Electrode Region. (a = 60 mils)

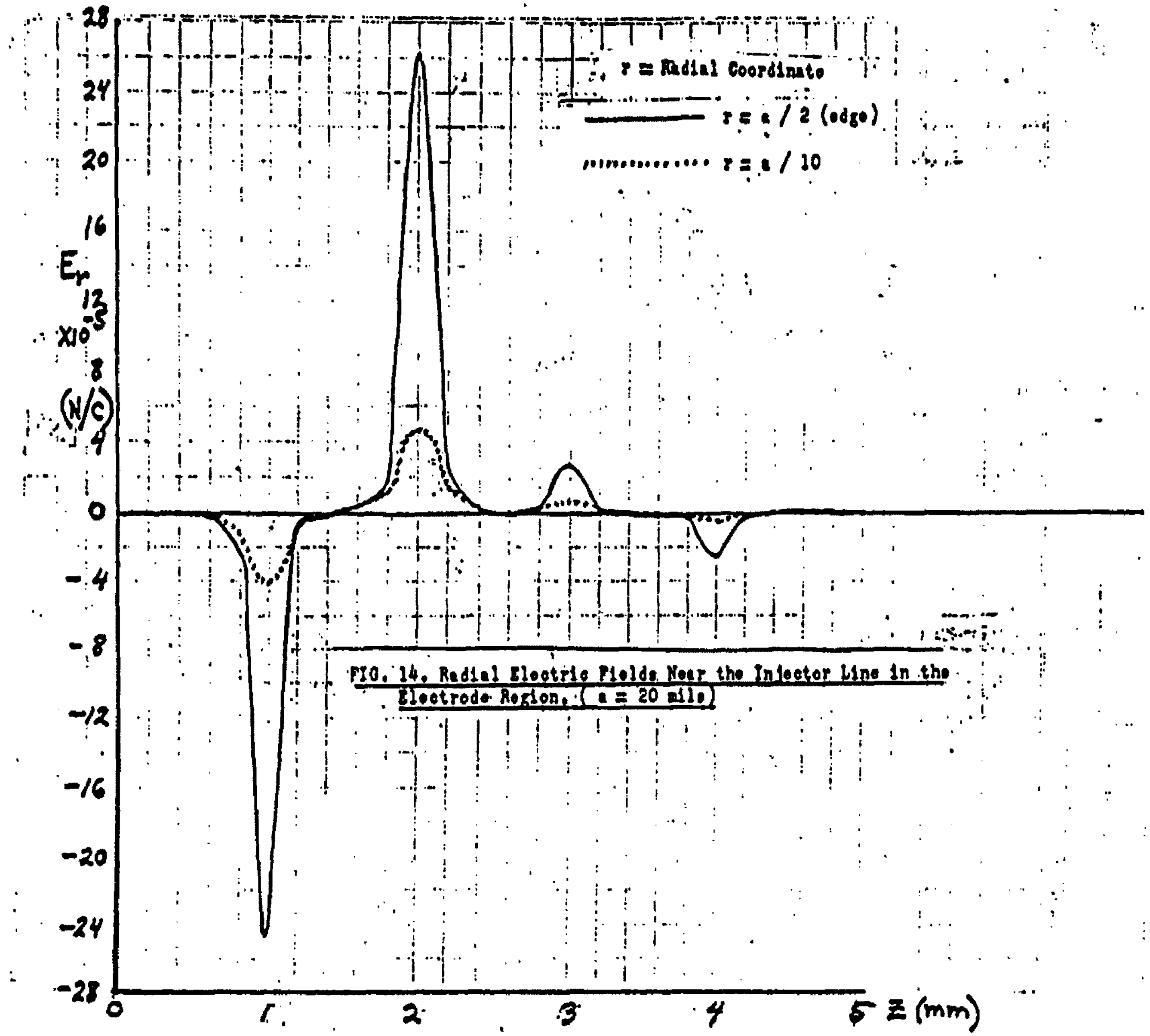

FIG. 14. Radial Electric Fields Near the Injector Line in the Electrode Region. (a = 20 mils)

FIG. 15. Radial Electric Field X 10^{-5} (N/C)
Hole Diameter = 1.50 mm (60 mils)

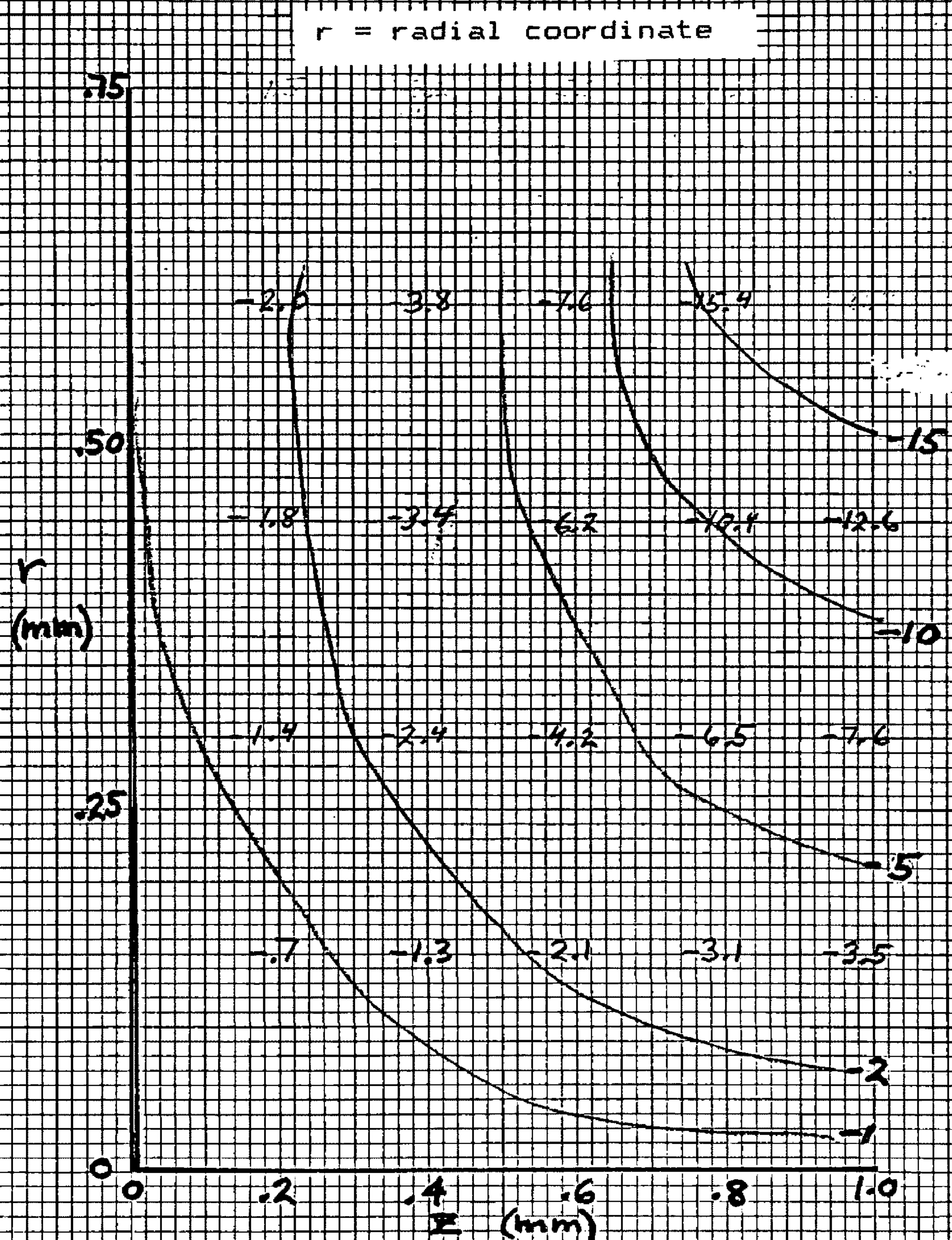

FIG. 16. Radial Electrice Field X 10^{-5} (N/C)
Hole Diameter = 0.5 mm (20 mils)

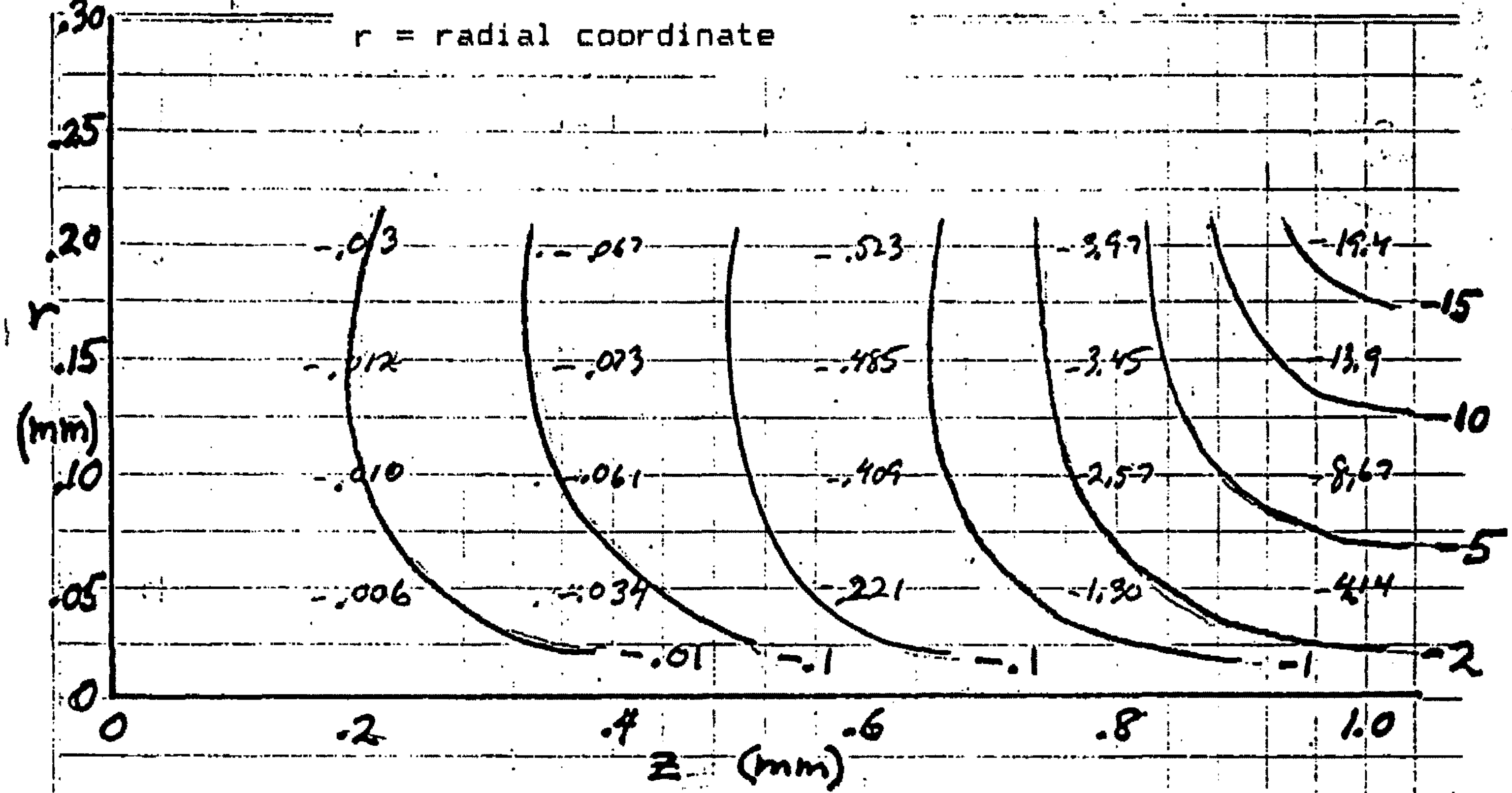

APPENDIX A

THE POISSON FIELD GENERATOR

The computer program POISSON is one of several programs comprising a package known as the POISSON/SUPERFISH group codes. These codes are used to calculate magnetostatic and electrostatic fields and to compute resonant frequencies and fields in radio-frequency cavities. POISSON is limited to problems having cylindrical or 2-dimensional symmetry. (Refer to the 1987 POISSON/SUPERFISH manual listed in the references.)

As a service to the user community, Los Alamos National Laboratory's Group AT-6 maintains and distributes a standard version of the codes. Source code, executable code, and examples are on the common file system at the Los Alamos Laboratory. The package can be accessed there or through ARPANET, or acquired on magnetic tape. Development of the codes began in the late sixties as the TRIM codes created by A. Winslow and J.Spoerl at the Lawrence Livermore National Laboratory. These FORTRAN 77 codes were expanded and improved there principally by Ronald Holsinger with theoretical assistance from Klaus Halbach. The work was financed partly by the U.S. Department of Energy and completed in 1975 at the Los Alamos Laboratory. The University of California operates the laboratory and holds the copyright.

Use of the program POISSON is facilitated by the use of 3 other programs from the package. A "POISSON run" consists of running the following four programs.

(1) AUTOMESH - Accepts a manually-prepared file specifying the geometry and potentials. Assigns mesh points and generates (x,y)-coordinates for straight lines, circular arcs, and segments of hyperbolas.

(2) LATTICE - Generates a triangular mesh from the list of mesh points and physical coordinates generated by AUTOMESH.

(3) POISSON - Solves Maxwell's electrostatic (magnetostatic) equations for the scalar (vector) potential for problems having 2-dimensional Cartesian or 3-dimensional cylindrical symmetry. Computes electric and magnetic fields.

(4) TEKPLOT - Plots the physical geometry and meshes generated by LATTICE and equipotential (or field) lines from POISSON.

A sample run is included which calculates and plots the electric field near the electrodes of the standard ion source. In that run, which was made on the University of Montana VAX, the four programs are called AUTSO, LATSO, POISO, and TEKSO, respectively.

In preparing the AUTSO (AUTOMESH) input, the user identifies the portions of the boundary having different potentials or current levels. For each such region, the user inputs the potential or current and the boundary of the region. The boundary input is a set of two-dimensional coordinates.

This was done for the AUTSO portion in the included example. In that part, the following inputs were coded into the file HFM4.DAT.

Run label.

NREG = Number of regions
DX = Horizontal mesh increment
DY = Vertical mesh increment
XMIN = Minumum horizontal coordinate
XMAX = Maximum horizontal coordinate
YMIN = Minimum vertical coordinate
YMAX = Maximum vertical coordinate
XREG1 = Location of mesh size change in the horizontal direction
KREG1 = Number of mesh points from XMIN to XREG1.
KMAX = Number of mesh points from XMIN to XMAX.
YREG1 = Location of first mesh size change in the vertical direction.

YREG2 = Location of second mesh size change in the vertical direction.

LREG1 = Number of mesh points from YMIN to YREG1.
LREG2 = Number of mesh points from YREG1 to YREG2.
LMAX = Number of mesh points from YMIN to YMAX.
NPOINT= Number of corners defining the boundary of the region.
Point specifications defining the boundary of the all-inclusive region. Note: in each region the corners (points) are either all read in in clockwise or all in in counterclockwise order.

Region specification for region 1:
CUR = Current level (amps) if it's a solenoid, voltage level (volts) if it's a static charged conductor.
MAT = Material code. A zero indicates that all interior points are omitted from the problem.
IBOUND= Boundary indicator. A zero indicates that field lines are parallel to the boundary. A one indicates that they are perpendicular to the boundary.
NPOINT= Number of PO entries (point specifications) for region 1.
Point specifications for region 1.
Region and point specification for regions 2, 3, and 4.

Each region or point specification must start and end with the symbol $.

Only the sample inputs are defined here, and many capabilities of the package are not mentioned. The file HFM4.DAT was prepared, AUTSO was started, and the filename

(HFM4) was given to AUTSO.

The inputs to LATSO (LATTICE) consist of the name of the file (TAPE73) containing the input generated by AUTSO, and some "CON-variables" to be used by LATTICE, POISSON, or TEKPLOT.

```
CON(19) = ICYLIN =1 cylindrical coordinates (X=r, Y=z)
CON(20) = NBSUP = Upper boundary field line parameter
CON(21) = NBSLO = Lower boundary field line parameter
CON(22) = NBSRT = Right boundary field line parameter
CON(23) = NBSLF = Left boundary field line parameter
```

These values were 0,0,1,1, respectively, indicating field lines parallel to the upper and lower boundaries and perpendicular to the left and right boundaries of the general region.

```
CON(46) = ITYPE = Symmetry type (A safe choice is
                  one(1), indicating no symmetry.)
CON(66) = XJFACT = 0. for all scalar potential problems.
                   (The decimal point is needed.)
```

The POISSON (POISO) run itself begins with the name of the input file or unit (TTY in the sample) and the dump number (zero (0) in the sample). POISSON accepts the list of mesh points in dump zero, a part of a large file generated by LATTICE.

```
CON(42) = KMIN = First radial mesh point
CON(43) = KTOP = Last radial mesh point
CON(44) = LMIN = First axial mesh point
CON(45) = LTOP = Last axial mesh point
CON(54) = XMIN = Radial coordinate for KMIN
CON(55) = XMAX = Radial coordinate for KTOP
CON(56) = YMIN = Axial coordinate for LMIN
CON(57) = YMAX = Axial coordinate for LTOP
```

The coordinates were set to 0., .5, 7.0, and 12. in the sample run and the pointers to 1, 11, 1, 26, respectively.

This specifies a cylindrical geometry containing the electrode holes, the region of interest. (See Figure 1.) The radius of the region is twice that of the holes and it's extent (5.0 mm) equals the axial distance through the three holes. The axial centerline of the mesh coincides with that of the holes.

In preparing input for these programs, decimal points are required as in the sample. Users must also be careful to enter the terminator (S) as shown.

POISSON solves the boundary value problem at the specified mesh points and indicates that dump number one has been written on the dump file. It then prompts the user with "? TYPE INPUT VALUE FOR DUMP NUM ". By entering -1 at this point, the user terminates the POISSON run.

If a plot of the field or equipotential lines is desired the user runs TEKPLOT (TEKSO). The inputs required are

```
NUM  = Dump number
ITRI = 0 for triangular mesh (=1 otherwise)
NPHI = Number of equipotential lines
```

A plot is included in the sample run. The POISSO run generated a file called OUTPOI which contains the electrode field in and around the electrode holes. This file was then input to SCHAR ion beam simulation code as discussed in Appendix B.

```
$ TYPE HFM4.DAT
RUN NO.3  20 MIL (.5MM) DIAMETER HOLE  14 JULY,1989
$REG NREC=4,DX=.0250,DY=.2,YMAX=19.,XMAX=7.,NPOINT=5,
XREC1=1.,KREC1=41,KMAX=101,
YREC1=7.,YREC2=12.,LREC1=36,LREC2=86,LMAX=111$
$PO Y=0.,X=0.$
$PO Y=19.,X=0.$
$PO Y=19.,X=7.$
$PO Y=0.,X=7.$
$PO Y=0.,X=0.$
$REG MAT=0,IBOUND=-1,CUR=5000.,NPOINT=9$
$PO Y=0.,X=0.$
$PO Y=1.,X=0.$
$PO Y=1.,X=6.$
$PO Y=7.,X=6.$
$PO Y=7.,X=.25$
$PO Y=8.,X=.25$
$PO Y=8.,X=7.$
$PO Y=0.,X=7.$
$PO Y=0.,X=0.$
$REG MAT=0,IBOUND=-1,CUR=-600.,NPOINT=5$
$PO Y=9.,X=7.$
$PO Y=9.,X=.25$
$PO Y=10.,X=.25$
$PO Y=10.,X=7.$
$PO Y=9.,X=7.$
$REG MAT=0,IBOUND=-1,CUR=0.,NPOINT=9$
$PO Y=11.,X=7.$
$PO Y=11.,X=.25$
$PO Y=12.,X=.25$
$PO Y=12.,X=6.$
$PO Y=18.,X=6.$
$PO Y=18.,X=0.$
$PO Y=19.,X=0.$
$PO Y=19.,X=7.$
$PO Y=11.,X=7.$
$ RUN AUTSO'

?TYPE INPUT FILE NAME
HFM4


REGION NO.  1
OK


REGION NO.  2
OK

REGION NO.  3

REGION NO.  4
OK
FORTRAN STOP
$ RUN LATSO

?TYPE INPUT FILE NAME
TAPE73
```

```
DUMP 0 WILL BE SET UP FOR POISSON

 RUN NO.3  20 MIL (.5MM) DIAMETER

?TYPE INPUT VALUES FOR CON(?)
*19 1 *21 0 0 1 1 *46 1 *66 0. S

ELAPSED TIME =   26.5 SEC.

ITERATION CONVERGED

ELAPSED TIME =   48.7 SEC.

GENERATION COMPLETED

DUMP NUMBER 0 HAS BEEN WRITTEN ON TAPE35.
FORTRAN STOP
$ RUN POISO

?TYPE "TTY" OR INPUT FILE NAME

TTY

?TYPE INPUT VALUE FOR DUMPNUM
0

BEGINNING OF POISSON EXECUTION FROM NUMBER 0

PROB. NAME = 20 MIL (.5mm) DIAMETER HOLE

?TYPE INPUT VALUES FOR CON (?)

*42  1 11  1 26 *54 0.  .5  7.  12.  s

   CYCLE       AMIN         AMAX      RESIDUAL-AIR  ETA-AIR  RHOAIR   XJFACT

     0      0.0000E+00   0.0000E+00   1.0000E+00   1.0000   1.9000   0.0000

    200                              RHOAIR OPTIMIZED   0.9865   1.9486   LAMBDA 1

    200    -5.9970E+02   4.9998E+03   1.6279E-03   0.9865   1.9486   0.0000
 UMT01::_TXB4: 19:05:41 POISO     CPU=00:01:58.52 PF=5164 IO=2244 MEM=1024

    400                              RHOAIR OPTIMIZED   0.9591   1.9487   LAMBDA 1

    400    -5.9970E+02   5.0000E+03   3.3151E-06   0.9591   1.9487   0.0000
 UMT01::_TXB4: 19:06:43 POISO     CPU=00:02:19.28 PF=5172 IO=2247 MEM=1024

    450    -5.9970E+02   5.0000E+03   4.3051E-07   0.9595   1.9487   0.0000

 SOLUTION CONVERGED IN  450 ITERATIONS

 ELAPSED TIME =  387.2 SEC.

 DUMP NUMBER  1 HAS BEEN WRITTEN ON TAPE35.
```

```
ELAPSED TIME  =  387.2 SEC.

DUMP NUMBER  1 HAS BEEN WRITTEN ON TAPE35.

?TYPE INPUT VALUE FOR DUMP NUM
-1
FORTRAN STOP
$ RUN TEKSO

?TYPE INPUT DATA- NUM, ITRI, NPHI, INAP, NSWXY,
1 0 25 S
INPUT DATA
NUM=  1     ITRI= 0     NPHI=  25     INAP= 0     NSWXY= 0

PLOTTING PROB. NAME = RUN NO.3  20 MIL (.5MM) DIAMETER     CYCLE=450

?TYPE INPUT DATA- XMIN, XMAX, YMIN, YMAX,
S
INPUT DATA
XMIN=    0.000  XMAX=    7.000  YMIN=    1.000  YMAX=  18.000

?TYPE GO OR NO
GO
```

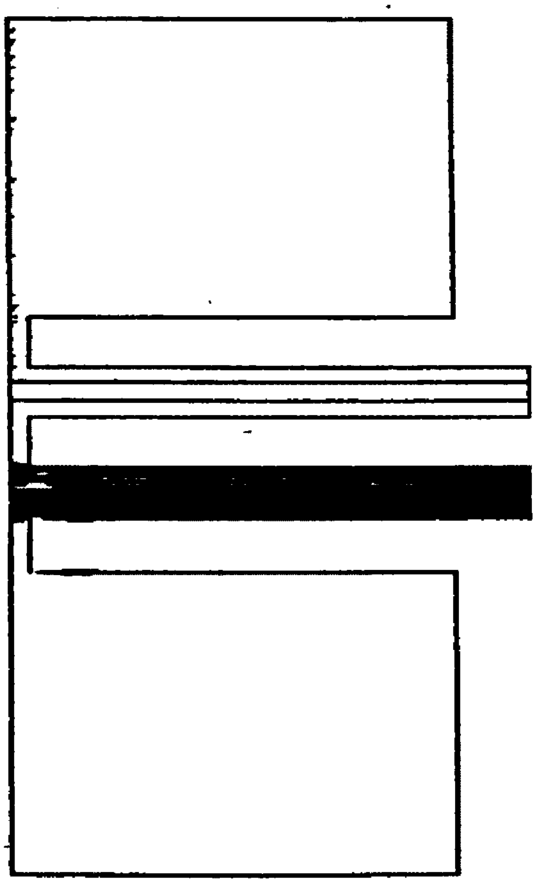

PROB. =RUN NO.3 20 MIL (.5MM) DIAMETER CYCLE = 450

APPENDIX B

SCHAR COMPUTER CODE FOR THE OPTICALLY PUMPED ION SOURCE

In 1987, Hayden and Jakobson modified their computer program SCHAR to study beam degradation in the LAMPF optically pumped ion source (Hayden,1987). The new version of SCHAR, known as SCHSL5, simulates the relevant features of the optically pumped ion source configuration described in the figures and table in section I. Given the field due to the electrode potentials, SCHSL5 can simulate the motions of protons injected into the first electrode hole, provided their initial conditions are known.

The output of SCHAR includes macrofilament count (NLEFT), emittances (SXVX,SYVY,...), rms transverse velocity components (VXRMS,VYRMS), rms transverse position components (XRMS,YRMS), and others. These variables are printed at key axial positions: at both sides of each electrode, at the reference point (z=61mm), at the neutralizer, after it, at the entrance to the ionizer,and following the ionizer.

Portions of a sample run are included. The run used the POISSON-generated electric field presented in Appendix A. That field results from a single 20-mil cylindrical hole in each electrode, the electrodes being 1 mm thick and mutually separated by 1 mm gaps. They have potentials 5kv, -.6kv, and 0kv respectively. The magnetic fields in the standard ion source are calculated in SCHSL5.

The sample run begins with an editor (TECO) session in order to locate the field values in POISSON's output file OUTPOI.LIS. (The field values began in line 146.)

Next, before SCHSL5 could be run, the electric field data required conversion to a form which would be compatible with SCHSL5. The program OPREAD was used for this purpose. The user-supplied inputs required by OPREAD were as follows.

Name of the output file (EMF, here)
N_x = No. of X-points (radial mesh points, here)
N_y = No. of Y-points (axial mesh points, here)
N_L = No. of lines in OUTPOI.LIS preceeding the electric field data (145,here).
E-field multiplier

In the sample, N_x= 11 AND N_y = 26. This causes OPREAD to extract a grid for an electric field which is cylindrical about the injector line and which has a diameter which is twice that of the hole diameter (.5mm) and which has a length extending through the electrode region (5mm).

Geometry input to AUTOMESH (Appendix A) was in millimeters; consequently, the electric field output by POISSON was in volts/mm. Since SCHSL5 requires that the electric field be in volts/m, the E-field multiplier was set at 1000.

```
$ TECO
ENTER FILE NAME
OUTPOI.LIS
OLD FILE

 3E505 CHARACTERS.
*[40LT\T\10T$$
1LEAST SQUARES EDIT OF PROBLEM , CYCLE   450

 NODE       SYMMETRY TYPE
O  K    L     V(SCALAR)        R            Z           ER  V /MM   EZ  V /MM   ET  V /MM

    1  36   4.99991E+03     0.00000      7.00000        0.000       0.218       0.214

    3  36   4.99992E+03     0.05000      7.00000       -0.084       0.121       0.143

    5  36   4.99992E+03     0.10000      7.00000       -0.135       0.036       0.143
*
FORTRAN PAUSE
$ RUN OPREAD
ENTER E-FIELD NAME
EM4
ENTER TOTAL NUMBER OF X-POINTS, TOTAL NUMBER OF Y-POINTS
11,26
ENTER NUMBER OF LINES TO BYPASS
146
ENTER E-FIELD MULTIPLIER---DEFAULT=1.0
1000
FORTRAN STOP
$ TYPE EM4.DAT
 10  25
  0   0  0.000000E+00  2.180000E+02
  1   0 -8.400000E+01  1.210000E+02
  2   0 -1.350000E+02  3.600000E+01
  3   0 -1.430000E+02 -8.800000E+01
  4   0 -7.900000E+01 -2.140000E+02
  5   0 -4.000000E+00 -4.200000E+02
  6   0  2.290000E+02 -1.600000E+02
  7   0 -3.300000E+01 -2.800000E+01
  8   0 -2.500000E+01 -1.800000E+01
  9   0 -4.100000E+01 -1.500000E+01
 10   0 -4.300000E+01 -1.100000E+01
  0   1  0.000000E+00  2.205000E+03
  1   1 -5.560000E+02  2.023000E+03
  2   1
```

The inputs to SCHAR are:

XOMAX = $\hat{X}$ = Maximum value of X at z=0
YOMAX = $\hat{Y}$ = Maximum value of Y at z=0
VXSMAX = $\hat{V}_x$ = Maximum value of $\dot{X}$ at z=0
VYSMAX = $\hat{V}_y$ = Maximum value of $\dot{Y}$ at z=0
VO = Particle speed at z=0
CONSQ = Interaction scale
NPART = N_o = Number of macroparticles
NSOL = Number of solenoids
BO = Strength of the axial magnetic field in the electrode region.
CELLEN = Length of neutralizer region
FLDLEN = Length of neutralizer solenoid field
NSTCEL = Number of integration steps in each cell.
NSTFLD = Number of integration steps in each cell in which the magnetic field is nonzero.
FRAC2 (not used)
FRACB (not used)
Third solenoid hole radius. (at ionizer entrance)
Picture option.
Particle 1 input override. (Allows non-random input for one particle.)
Overriding lengths for neutralizer, ionizer, and drift region. (These override file input of lengths.)
Number of integration steps for those regions.
Random number generator seed.
Number of holes per electrode.
INDEP indicates one (centered) hole per electrode.
Initial condition selector.
CR selects a KV distribution for position and
P selects a KV distribution for position and a parabolic distribution for velocity.
Name of the input file containing the electric field.
Hole separation control (for multiple holes per electrode)
Number of regions in the electrode structure.
ICUT = Number of run-repititions for estimating the final beam current.
Number of integration steps in the 5 regions in the electrode region.
Lengths of the 5 regions (1mm in the sample).
DELR = radial integration step size for electrode regions.
DELZ = axial integration step size for electrode regions.

Upon the last entry, tables labelled "RESULTS AFTER SOLENOID # 0" are printed. After integrating through successive cells, the tables are printed for the other critical axial locations. With N =1000, the entire run (replications included), sometimes required several hours on the VAX8600.

At each selected axial location the table shows the status of the particle population at that location. The number of particles is indicated and the average and rms angular momenta are shown.

The "QQ MATRIX" is the correlation matrix of X,X$'$,Y,and Y$'$ normalized by their maximum values specified in the input.

$$QQ(I,J) = \left(\sum_{K=1}^{N} (Q_I(K) - \bar{Q}_I)(Q_J(K) - \bar{Q}_J) / (N\hat{Q}_I\hat{Q}_J)\right)\gamma$$

where Q_I = Ith. variable,

$\bar{Q}_I$ = Mean value of Q_I,

$\hat{Q}_I$ = Initial maximum of Q_I,

(I = 1,2,3,4)

N_o = Number of macroparticles left, and

γ = 1 for non-relativistic speeds.

The quantity "VOL4" is the volume of an ellipsoid representing the swarm of N points in 4 dimensional space:

$$VOL4 = (4\pi)^2\sqrt{|QQ|}\ /2$$

Six phase space areas are then printed - SXVX, SYVY, SXVY, SYVX, SXY, and SVSVY. These are computed from QQ. For example,

$$SXY = 4\pi\sqrt{QQ(1,1)*QQ(3,3)-QQ(1,3)*QQ(3,1)}$$

SX-EMITTANCE and SY-EMITTANCE are the emittances corresponding to the phase space areas SXVX and SYVY respectively:

$$SX = SXVX*XOMAX*VSXMAX*(10^6/\bar{V}_z)/\pi$$
$$SY = SYVY*YOMAX*VSYMAX*(10^6/\bar{V}_z)/\pi$$

The other outputs are

EXVX, EYVY, and EXY -- convex polygon areas (not used)
NEDGEX, NEDGEY, and NEDGXY -- not used
THETA -- not used
Z -- z coordinate (m)
XAVE, YAVE -- mean transverse position coordinates
VXAVE, VYAVE -- mean transverse velocity coordinates
SPAVE -- mean speed
XRMS, YRMS -- rms transverse position coordinates
VXRMS, VYRMS -- rms transverse velocity coordinates
SPRMS -- rms speed
TUNANG -- tuning angle (not used)

"AVERAGE SPHERE RADIUS" and "SPHERE RADIUS RMS" refer to the mean and rms values of

$$\sqrt{(X/\hat{X})^2 + (V_x/\hat{V}_x)^2 + (Y/\hat{Y})^2 + (V_y/\hat{V}_y)^2}$$

respectively.

```
$ RUN SCH6L5
ENTER "FILE" TO READ IN DATA FILE
FILE
ENTER FILE NAME
TRY4
ENTER "CHANG" TO CHANGE FILE CONTENT,"/" FOR PRINTOUT
CHANG

CHANGE INPUT DATA-CARRIAGE RETURN SAYS NO CHANGE
XOMAX= 2.500E-04   NEW VALUE=
YOMAX= 2.500E-04   NEW VALUE=
VXSMAX= 3.000E+04   NEW VALUE=
VYSMAX= 3.000E+04   NEW VALUE=
VO= 1.600E+05   NEW VALUE=
CONSQ= 1.000E-03   NEW VALUE=
CURR= 0.000E+00   NEW VALUE=.000125
NPART=1000   NEW VALUE=
NSOL=    3   NEW VALUE=
BO= 1.560E+00   NEW VALUE=
CELLEN= 1.000E-01   NEW VALUE=
FLDLEN= 1.000E-01   NEW VALUE=
NSTCEL=  16   NEW VALUE=
NSTFLD=  16   NEW VALUE=
FRAC2= 5.000E-01   NEW VALUE=
FRACB= 0.000E+00   NEW VALUE=
CHANGES MADE. ENTER "FILE" TO WRITE NEW FILE

ENTER 3RD SOLENOID HOLE RADIUS IN METERS. DEFAULT 1 M.
.00714
ENTER "POP" FOR PICTURE OPTION.

ENTER "OR" FOR PARTICLE #1 INPUT OVERRIDE

ENTER "C" FOR OVERRIDING CELL LENGTH
C
```

```
CELLEN( 1)=.112
NST( 1)=16
CELLEN( 2)=.0965
NST( 2)=16
CELLEN( 3)=.632
NST( 3)=8
ENTER RANDOM NUMBER SEED FOR FIRST RUN

87
FILE NAME FOR SAVED FILE--START WITH X--IS XGM
ENTER "INDEP" FOR 1 HOLE, "CL7" FOR 7 HOLES, "CL19"FOR 19 HOLES
"CL13" FOR 13 HOLE STAR, "CL37" FOR 37 HOLES, "SLOTS" FOR SLOTS IN CIRCLE
"RING" FOR RING INPUT
INDEP
ENTER "P" FOR A PARABOLIC V DISTRIBUTION

ENTER NAME OF E-FILE
EM4
ENTER C TO C HOLE SEPARATION. 0. GIVES DEFAULT TO ORIGINAL.


VZSMAX SET BY ENERGY AT  1.4188281E+03

ENTER NUMBER OF REGIONS IN SOURCE--5 MAX.
5
ENTER CUTOFF NUMBER FOR PARTICLES FOUND
146
# OF STEPS IN REGION 1 =10
# OF STEPS IN REGION 2 =10
# OF STEPS IN REGION 3 =10
# OF STEPS IN REGION 4 =10
# OF STEPS IN REGION 5 =10
```

```
LENGTH OF REGION 1 (IN METERS)=.001
LENGTH OF REGION 2 (IN METERS)=.001
LENGTH OF REGION 3 (IN METERS)=.001
LENGTH OF REGION 4 (IN METERS)=.001
LENGTH OF REGION 5 (IN METERS)=.001
ENTER DELR,DELZ IN METERS
.000050,.0002
ENTER "P" FOR PIKTUR



******************************************************************************
RESULTS AFTER SOLENOID #  0                        ISTART=          87   RUN # 1
******************************************************************************

REGION # 0   STEP # 0   ANG.MOM.=-1.593E-01   RMS ANG. MOM.= 2.608E+00

1000 PARTICLES LEFT IN THE BEAM

NUMBER OF CLOSE ENCOUNTERS=       0

                             QQ MATRIX
 2.640E-01 -1.362E-02  3.264E-03 -1.720E-02
-1.362E-02  2.526E-01  3.577E-03  3.655E-03
 3.264E-03  3.577E-03  2.421E-01 -5.754E-03
-1.720E-02  3.655E-03 -5.754E-03  2.447E-01

VOL4= 4.9425073E+00
SXVX= 3.2409458E+00   SYVY= 3.0577972E+00
SXVY= 3.1869431E+00   SYVX= 3.1073506E+00
SXY= 3.1765304E+00    SVXVY= 3.1244259E+00
SIGMAS= 2.4328848E-02
EXVX= 0.0000000E+00   EYVY= 0.0000000E+00   EXY= 0.0000000E+00
NEDGEX=  0            NEDGEY=  0            NEDGXY=  0
```

```
SX-EMITTANCE= 4.879E+01 MM-MR   SY-EMITTANCE= 4.603E+01 MM-MR
EX-EMITTANCE= 0.000E+00 MM-MR   EY-EMITTANCE= 0.000E+00 MM-MR
THETA=   0.00 DEG.
XAVE= 2.540E-06    XRMS= 1.285E-04
YAVE=-3.124E-06    YRMS= 1.231E-04
Z= 0.0000000E+00
VXAVE=-5.229E+02   VXRMS= 1.509E+04
VYAVE=-7.246E+02   VYRMS= 1.485E+04
SPAVE= 1.6000000E+05    SPRMS= 6.0515366E-03
TUNE ANGLE=     0.00 DEG.     DIFF. ANGLE=   0.00 DEG.
AVERAGE SPHERE RADIUS= 9.787E-01   SPHERE RADIUS RMS= 2.165E-01

NUMBER OF PARTICLES IN RING # 1=1000   REL. DENS.= 4.0000
NUMBER OF PARTICLES IN RING # 2=   0   REL. DENS.= 0.0000
NUMBER OF PARTICLES IN RING # 3=   0   REL. DENS.= 0.0000
NUMBER OF PARTICLES IN RING # 4=   0   REL. DENS.= 0.0000
NUMBER OF PARTICLES IN RING # 5=   0   REL. DENS.= 0.0000
NUMBER OF PARTICLES IN RING # 6=   0   REL. DENS.= 0.0000
NUMBER OF PARTICLES IN RING # 7=   0   REL. DENS.= 0.0000
NUMBER OF PARTICLES IN RING # 8=   0   REL. DENS.= 0.0000
NUMBER OF PARTICLES IN RING # 9=   0   REL. DENS.= 0.0000
NUMBER OF PARTICLES IN RING #10=   0   REL. DENS.= 0.0000
   0 PARTICLES LOST

EKIN= 1.2799971E+10 EPOT= 1.6369467E+08 ETOT= 1.2963666E+10
```

```
*******************************************************************************
RESULTS AFTER SOLENOID #   0                ISTART= 87    RUN # 1
*******************************************************************************

REGION # 0, STEP # 0  ANG.MOM =.05097   RMS ANG.MOM= 2.272

 664 PARTICLES LEFT IN THE BEAM

NUMBER OF CLOSE ENCOUNTERS=    12925

                                QQ MATRIX
 1.361E-01 -6.485E-01 -1.897E-03  1.257E-02
-6.485E-01  3.395E+00  5.545E-03 -5.565E-02
-1.897E-03  5.545E-03  1.480E-01 -6.947E-01
 1.257E-02 -5.565E-02 -6.947E-01  3.538E+00

VOL4= 3.2565837E+00
SXVX= 2.5560253E+00    SYVY= 2.5514195E+00
SXVY= 8.7174206E+00    SYVX= 8.9087534E+00
SXY= 1.7832688E+00     SVXVY= 4.3548969E+01
SIGMAS= 5.9998488E+00
EXVX= 0.0000000E+00    EYVY= 0.0000000E+00    EXY= 0.0000000
NEDGEX=   0            NEDGEY=   0            NEDGXY=   0
SX-EMITTANCE= 1.979E+01 MM-MR    SY-EMITTANCE= 1.976E+01MM-MR
EX-EMITTANCE= 0.000E+00 MM-MR    EY-EMITTANCE= 0.000E+00MM-MR
THETA=    0.00 DEG.
XAVE= 1.291E-07     XRMS= 9.228E-05
YAVE=-2.184E-06     YRMS= 9.626E-05
Z= 1.0000000E-03
VXAVE=-8.795E+02    VXRMS= 5.532E+04
VYAVE= 1.817E+03    VYRMS= 5.647E+04
SPAVE= 3.1841963E+05    SPRMS= 5.6239014E+03
TUNE ANGLE=    0.00 DEG.    DIFF. ANGLE=    0.00 DEG.
AVERAGE SPHERE RADIUS= 2.520E+00   SPHERE RADIUS RMS= .9330

NUMBER OF PARTICLES IN RING # 1= 664   REL. DENS.= 2.6560
NUMBER OF PARTICLES IN RING # 2=   0   REL. DENS.= 0.0000
NUMBER OF PARTICLES IN RING # 3=   0   REL. DENS.= 0.0000
NUMBER OF PARTICLES IN RING # 4=   0   REL. DENS.= 0.0000
NUMBER OF PARTICLES IN RING # 5=   0   REL. DENS.= 0.0000
NUMBER OF PARTICLES IN RING # 6=   0   REL. DENS.= 0.0000
NUMBER OF PARTICLES IN RING # 7=   0   REL. DENS.= 0.0000
NUMBER OF PARTICLES IN RING # 8=   0   REL. DENS.= 0.0000
NUMBER OF PARTICLES IN RING # 9=   0   REL. DENS.= 0.0000
NUMBER OF PARTICLES IN RING #10=   0   REL. DENS.= 0.0000
 336 PARTICLES LOST

EKIN= 5.0711417E+10 EPOT= 2.3878605E+08 ETOT= 5.0950201E+10
```

```
*****************************************************************************
RESULTS AFTER SOLENOID #  3                         ISTART = 87   RUN # 1
*****************************************************************************

REGION # 3, STEP # 4  ANG.MOM= -.3304  RMS ANG.MOM=.5373

   6 PARTICLES LEFT IN THE BEAM

                                     QQ MATRIX
  3.290E+02  3.884E+00  1.117E+02  1.260E+00
  3.884E+00  4.589E-02  1.303E+00  1.468E-02
  1.117E+02  1.303E+00  1.417E+02  1.633E+00
  1.260E+00  1.468E-02  1.633E+00  1.881E-02

 VOL4= 8.1901103E-03
 SXVX= 1.1384976E+00   SYVY= 2.9859206E-01
 SXVY= 2.6956205E+01   SYVX= 2.7541679E+01
 SXY= 2.3215642E+03    SVXVY= 3.1978080E-01
 SIGMAS= 3.5153671E+02
 EXVX= 0.0000000E+00   EYVY= 0.0000000E+00   EXY= 0.0000000
 NEDGEX=  0            NEDGEY=  0            NEDGXY=  0
 SX-EMITTANCE= 2.742 MM-MR   SY-EMITTANCE= .7188 MM-MR
 EX-EMITTANCE= 0.000 MM-MR   EY-EMITTANCE= 0.000 MM-MR
 THETA=   0.00 DEG.
 XAVE=-1.348E-03    XRMS= 4.967E-03
 YAVE=-1.205E-03    YRMS= 3.260E-03
 Z= 8.4550011E-01
 VXAVE=-1.836E+03   VXRMS= 7.040E+03
 VYAVE=-1.640E+03   VYRMS= 4.507E+03
 SPAVE= 9.9173850E+05    SPRMS= 4.7843137E+02
 TUNE ANGLE=    0.00 DEG.    DIFF. ANGLE=   0.00 DEG.
 AVERAGE SPHERE RADIUS= 2.252E+01   SPHERE RADIUS RMS= 4.010

 NUMBER OF PARTICLES IN RING # 1=   0   REL. DENS.= 0.0000
 NUMBER OF PARTICLES IN RING # 2=   0   REL. DENS.= 0.0000
 NUMBER OF PARTICLES IN RING # 3=   1   REL. DENS.= 0.0008
 NUMBER OF PARTICLES IN RING # 4=   5   REL. DENS.= 0.0029
 NUMBER OF PARTICLES IN RING # 5=   0   REL. DENS.= 0.0000
 NUMBER OF PARTICLES IN RING # 6=   0   REL. DENS.= 0.0000
 NUMBER OF PARTICLES IN RING # 7=   0   REL. DENS.= 0.0000
 NUMBER OF PARTICLES IN RING # 8=   0   REL. DENS.= 0.0000
 NUMBER OF PARTICLES IN RING # 9=   0   REL. DENS.= 0.0000
 NUMBER OF PARTICLES IN RING #10=   0   REL. DENS.= 0.0000
  994 PARTICLES LOST

 EKIN= 4.9177677E+11 EPOT= 0.0000000E+00 ETOT= 4.9177677E+11
```

```
                SUMMARY OF EMITTANCE VALUES
SOL #         SXVS              SYVY              SAVE

     0   4.8159080E+00    4.6929975E+00    4.7544527E+00
     1   1.1659292E+01    1.1700906E+01    1.1680099E+01
     2   5.7025990E+01    4.7932362E+01    5.2479176E+01
     3   1.1384976E+00    2.9859206E-01    7.1854484E-01
IRUN= 1 ISTART=              87 IWRITE=  6 CURNEW= 7.500E-07
    6
NLEFT= 114
IRUN= 2 ISTART=-1926247624 IWRITE= 10 CURNEW= 6.250E-07
   10
NLEFT= 134
IRUN= 3 ISTART=   -26875723 IWRITE= 16 CURNEW= 6.667E-07
   16
NLEFT= 140
IRUN= 4 ISTART= 1346569940 IWRITE= 19 CURNEW= 5.938E-07
   19
NLEFT= 145
IRUN= 5 ISTART=-1048369881 IWRITE= 24 CURNEW= 6.000E-07
   24
NLEFT= 137
IRUN= 6 ISTART= -201476605 IWRITE= 27 CURNEW= 5.625E-07
   27
NLEFT= 142
IRUN= 7 ISTART=-1116682529 IWRITE= 38 CURNEW= 6.786E-07
   38
  Interrupt
```

REFERENCES

Hayden, R.J. and Jakobson, M.J., The Space Charge Computer Program SCHAR. (Preprint) Dept. of Physics and Astronomy, University of Montana, 59812. (1987)

Hayden, R.J. and Jakobson, M.J., Univ. of Montana.
van Dyck, .O.B. and York, R.L., Los Alamos National Laboratory. Beam Dynamics Calculations for the LAMPF Optically Pumped Ion Source. (Preprint) (1989)

Jakobson, M.J. and Hayden, R.J., Nuclear Instruments and Methods A258 536-541, North-Holland, Amsterdam (1987).

Jakobson, M.J. and Hayden, R.J., Macrofilament Simulation of High Current Beam Transport. IEEE NS#4, P2540 (1983)

Kapchinskij, M. and Vladimiskij, V.V., Conference on High Energy Accelerators and Instrumentation, CERN, Geneva (1959).

Lawson, J.D. The Physics of Charged Particle Beams. Clarendon Press. Oxford, England. (1977)

POISSON/SUPERFISH Reference Manual LA-UR-87-126. Los Alamos Accelerator Code Group MS H829. Los Alamos, New Mexico, 87545. Jan.1, 1987.

York, R.L., Dulick, M., Cornelius, W.D., van Dyck, O.B., Proceedings of the International Workshop on Hadron Facility Technology, Feb. 1987.